November 3, 1967

Mailing Address

STAT

[redacted]

Enclosed are four copies of one technical report on the subject contract:

Task 4 Calibration

One copy of the report has been sent directly to Bill R. Reports on task 2 and 3, were previously submitted on September 19, 1967. The report on Task 1 is in draft typing and will be submitted shortly.

Very truly yours,

[redacted]

STAT

Declass Review by NGA.

S 75087

October 31, 1967

INVOICE #1067-06-23

For Services Rendered on Contract [redacted] STAT

STAT From: [redacted]

To: U. S. Government

STAT [redacted]

Technical Representative of Contracting Officer

November 15, 1967

Letter Progress Report #6, Contract [redacted] STAT

This report covers the period from 1 Oct 67 to 15 Nov 67.

The final technical report on Task 4 "Calibration" was submitted. Task 4 is complete. It was concluded that a simple calibration device was needed and could be made for determining the accuracy of the High Precision Stereo Comparator and other comparators. It was recommended that preliminary design be initiated.

The final technical report on Task 1 "the Necessary Accuracy" was submitted. Task 1 is complete. It was concluded that the least count of existing machines is adequate for most measuring requirements and the proposed least count of the High Precision Stereo Comparator is adequate for all measuring tasks. It was also concluded that extreme accuracy is required only for measuring very short lengths, less than 1cm. Determination of flying height appears to be the dominant error for longer measurements. It was recommended that further work be done to search out other dominant error sources and attempt to reduce their errors. It was also recommended that the criteria for a simplified machine be established.

Work on this contract is complete.

[redacted] STAT

STAT

Task 3
Contribution of Film Distortion

Research Effort in Support of
High Precision Stereo Comparator

Approved For Release 2005/05/20 : CIA-RDP78B04770A001500040016-6

AD 5150 87

STAT

[redacted]

September 19, 1967

STAT [redacted]

Enclosed are four copies each of two technical reports on the subject contract:

(a) Task 2 The Contribution of Stereo

(b) Task 3 The Contribution of Film Distortion

One copy of each report has been sent directly to Bill R. Reports on Task 1 and Task 4 will be submitted next month.

Very truly yours,

[redacted] STAT

[redacted] STAT

September 18, 1967

STAT [redacted]

RESEARCH EFFORT IN SUPPORT OF
HIGH PRECISION STEREO COMPARATOR

Task 3 the Contribution of Film Distortion

Work Statement: It appears that the problem most appropriate for initial consideration is a thermal one. We will therefore concentrate our attention in this task on a heat balance model.

We will establish an analytical heat balance model, transient and steady state, for film which is vacuum clamped to a glass platen and illuminated with high intensity light.

A literature search will be made for experimental data on various film coefficients at various optical densities such as:

a) Thermal coefficient of expansion of film and variation with humidity.

b) Thermal conductivity of film.

c) Emissivity and view factor of film.

d) Convective heat transfer coefficient.

Where coefficients are not reported, we will attempt to derive an estimated value from known related technology. We anticipate it will be possible to establish an analytical expression for the two-dimensional transient temperature distribution in the film as affected by the above coefficient and:

a) Ambient temperature and humidity changes.

b) Absorption of radiation from the light source.

c) Cooling jets of air.

Submitted by:

[redacted] STAT

STAT

September 18, 1967

RESEARCH EFFORT IN SUPPORT OF HIGH PRECISION STEREO COMPARATOR

Task 3 the Contribution of Film Distortion

Contents

List of Figures

List of Tables

Approved For Release 2005/05/20 : CIA-RDP78B04770A001500040016-6

1. SUMMARY AND CONCLUSIONS

The various coefficients essential to constructing an analytical heat balance model were found in the literature, and are reported herein, with two exceptions. The exceptions were the dynamic characteristics of film expansion due to humidity changes and the dynamic characteristics of film expansion due to thermal changes. We have found no source for such data and we recommend that the dynamic characteristics be measured.

A two-dimensional transient analytical heat balance model was constructed and the equations are presented herein. The hand calculation of a numerical solution of the two-dimensional transient heat flow equations are not economically feasible. The numerical solution must be programmed for a high speed digital computer. A computer solution will yield temperature-time histories and dimensional changes of a grid of points on the two-dimensional film. We recommend that a computer program be prepared.

A one-dimensional steady state analytical heat balance model was constructed. This is a simplified approximation of the two-dimensional transient model and is amenable to hand calculation. In order to obtain an indication as to whether or not distortion is significant, some numerical examples were computed of the one-dimensional steady state model. The numbers were based on the expected values for the High Precision Stereo Comparator as they are known at present. For low magnifications (3/4 $in.^2$ illuminated area) and conventional forced air cooling the temperature rise was computed to be 111^oF and film distortion across the illuminated area to be 0.42 millimeters. This is unacceptable. It gets worse as the magnification increases. At the highest magnification (0.03 in^2 illuminated area) and with conventional forced air cooling, the temperature rise was computed to be $2.5x10^{3o}F$. Such a temperature rise is completely unacceptable.

In a search for alternatives, cooling the film by sonic jet was considered. It was necessary to derive the heat transfer coefficient for the sonic jet cooling and the derivation is presented herein. For the 3/4 $in.^2$ illuminated area, the temperature rise was computed to be 14.5°F and distortion about 0.2 microns which is acceptable. F or the 0.0300 $in.^2$ illuminated area, the temperature rise was computed to be 215°F which is unacceptable. The above figures were based on use of a 500 watt xenon compact arc lamp in the High Precision Stereo Comparator with 8 watts of radiation being absorbed by the film at the film plane. The value 8 watts is open to serious question. It could easily be off by a factor of 4 or more in either direction. An experimental investigation is recommended to measure the heat flux at the film gate. We recommend that measurements be made on existing measuring engines and the results extrapolated to the High Precision Stereo Comparator.

Use of a sonic jet for cooling is undesirable. The jet would produce a high noise level and the momentum exchange at the film plane would introduce vibration into the film platen and the measuring engine structure.

It is evident that the thermal distortion problem is undoubtedly serious. We recommend that a numerical solution of the two-dimensional transient model be urgently pursued to determine tolerable radiation flux levels at the film plane. The program can then be used to predict over all film distortion and corrections introduced to compensate measuring inaccuracies.

2. FILM DISTORTION

The contribution of film distortion to measuring accuracy of the high precision stereo comparator is of prime importance. Film distortion generally results from changes in humidity, temperature, and age.

In any discussion of film distortion it is important to distinguish between the different types of dimensional change which may occur. Dimensional changes in film are of two types, temporary and permanent. The temporary dimensional changes are reversible and are usually repeatable. The permanent dimensional changes are irreversible.

2.1 TEMPORARY DIMENSIONAL CHANGES

(a) Thermal Expansion and Contraction

In heating and cooling of materials expansion and contraction occur. At constant relative humidity, film dimension expands and contracts as in other materials when temperature increases and decreases.

(b) Humidity Expansion andContraction

When the film base and emulsion take up moisture they swell and when they lose moisture, they contract. The magnitude of this effect is greater with emulsion coated film than with uncoated base because the emulsion has a greater tendency to contract than the base as the relative humidity is lowered. The base is compressed slightly by the emulsion under these conditions, thus increasing the contraction of the film at lower relative humidities. The humidity expansion and contraction of film follows the change in moisture content, so that dimensions at any given instant vary with the relative humidity of the atmosphere.

2.2 PERMANENT DIMENSIONAL CHANGES

All photographic films undergo gradual permanent size changes before use as a result of photographic processing and during subsequent aging of the processed films. The rate of permanent dimensional change for a particular film depends on the conditions under which it is used, processed and stored. The causes of permanent film distortion are:

(a) Loss of residual solvent and plasticizer
(b) Plastic flow of the base
(c) Release of the mechanical strain
(d) Mechanical effects of the gelatin.

The detail discussions of these causes are given in References 1 through 4.

2.3 FILM DISTORTION DURING A MEASUREMENT PERIOD

The most important film dimensional change is that which contributes to measuring error during a measurement period: the reversible thermal distortion. The radiative heat load from the light source can cause considerable film distortion. Dimensional changes during a measurement period due to other causes are expected to be negligible because:

1. The relative humidity of air surrounding the machine will be reasonably constant during a mearurement period.
2. The permanent size change during a measurement period is not likely to be any measurable amount.

In the present task, the effort will be directed toward the thermal effect. Various thermal coefficients that are important to the study of transient and steady-state heat balance of film have been surveyed and are discussed in the next section.

3. COEFFICIENTS

A literature survey has been conducted to obtain various coefficients and physical properties of photographic films. These coefficients and property values are required for an analytical transient heat balance model and calculating dimensional changes of a two dimensional film.

Most of the film property values can be found in References 1 and 4 except the transient thermal and humidity coefficients and the convective turbulent heat transfer coefficients of the cooling jet. The heat transfer coefficients of the cooling jet are important in the solution of the heat balance model, therefore they are derived in this report.

3.1 THERMAL CONDUCTIVITY

The thermal conductivity coefficients are expressed in BTU/(Hr)(SqFt)(Degree F per Ft). Reverence 1 shows the following values for

Kodak Plus-X Aercon Film (Triacetate thin base)Type 8402 (70-160F)	0.13
Kodak Plus-X Aerial Film (Estar thin base) Type 4401 (70-160F)	0.14

The thermal conductivity coefficients for the triacetate and Estar base materials are almost the same.

3.2 HEAT CAPACITY

The heat capacity of a material is expressed in a unit of BTU/lb/Degree F. Reference 1 lists the heat capacity of various films. The range of heat capacity is from 0.33 to 0.44 BTU/lb/Degree F.

3.3 SPECIFIC WEIGHT

The specific weight values for cellulose triacetate base and Estar base are 79.8 and 86.6 lb/cu ft respectively.

3.4 THERMAL AND HUMIDITY COEFFICIENTS OF LINEAR EXPANSION

The thermal and humidity coefficients of linear expansion for different film base materials are given in Reference 1. The coefficients are different in lengthwise and widthwise directions for cellulose acetate, Butyrate base and cellulose triacetate base. Estar base has the same coefficients in all directions.

The thermal and humidity coefficients of linear expansion for a number of Kodak films are listed in Table 1.

3.5 KENETIC COEFFICIENTS OF FRICTION

During a measurement period the film is vaccum clamped to a glass platen. Any movement of film due to the change of thermal environment will be resisted by the friction force

TABLE I

APPROXIMATE DIMENSIONAL CHANGE
CHARACTERISTICS OF KODAK AERIAL FILMS

FILM TYPE	Humidity Coefficient of Linear Expansion. % per 1% RH (Unprocessed).[1] Length	Width	Thermal Coefficient of Linear Expansion, % per Degree F.[2] Length	Width
Kodak Plus-X Aerecon Film, Type 8401, Cellulose, Triacetate, Base-Thickness .0052.	.0055	.0070	.0025	.0035
Kodak Plus-X Aerecon Film, (Thin Base) Type 8402, Cellulose, Triacetate Base-Thickness .00275	.0080	.0100	.0025	.0035
Kodak Plus-X Aerial Film, (Estar Thin Base) Type 4401, Estar Base, Base-Thickness .0025.	.0035	.0035	.0015	.0015
Kodak Special Plux-X Aerial Film (Estar Base), Type SO 135, Base-Thickness .0040.	.0025	.0025	.0015	.0015
Kodak Special Aerial Duplicating Film (Estar Thick Base), Type SO-117 Estar Base, Base-Thickness .0070.	.0015	.0015	.0015	.0015
Kodak Plus-X Aerographic Film Type 5401, Cellulose Acetate, Butyrate Base-Thickness .0052.	.0070	.0075	.0042	.0044

1. Measurements made at 70F between 20 and 70% RH for cellulosic films, and between 15 and 50% RH for Estar base films.

2. Measurements made at 20% RH between 70 and 120F.

resulting from the vaccum clamp action. To assess the total film distortion it is necessary to obtain the strain distribution in the film base. The resultant strain pattern of the film base is a combination of thermal expansion and friction effect.

Reference 1 lists the kinetic coefficients of friction for films against different materials. These values are duplicated and shown in Table II.

The surface condition of the galss platen will probably be similar to the smoothness of high polish chrome material. The range of kinetic coefficient of friction for high polish chrome material against film is between 0.1 and 0.35. The same coefficient range may be assumed for film against the glass palten.

3.6 EMISSIVITY

Neither Reference 1 nor Reference 2 lists the film emissivities. Emissivities for various material are tabulated in Reference 5. If the film surface condition be considered similar to glass or lacquer the emissivity range will be between 0.90 to 0.97.

The emissivity coefficients are required in the calculation of radiative heat rejection from the film surface to the surrounding medium. If the film temperature is low this heat loss quantity can be neglected.

3.7 COOLING JET TURBULENT CONVECTIVE HEAT TRANSFER COEFFICIENTS ON FILM

When film is subjected to illumination of high intensity, not only will the film change size but it also may be damaged or ignited. In section 5 of this report the numerical examples indicate the severeness of heating of film under high heat flux. It is almost sure that the cooling of film for the high precision stereo comparator will necessitate a high speed sonic air jet. Conventional blower type air cooling system usually

TABLE II

KINETIC COEFFICIENTS OF FRICTION

FILM PRODUCT:	Plus-X Aerecon Film, (Thin Base) Type 8402		Plus-X Aerecon Film Type 8401	Plus-X Aero-graphic Film Type 5401
FILM SURFACE:	Emul-Sion	Gelatin Backing	Back (Support)	Back (Support)
MATERIAL				
Anodized Aluminum Fine-finish 63 micro-inches, rms.	0.35	0.30	0.60	0.45
Aluminum, Fine-finish 63 microinches, rms.	0.45	0.40	0.55	0.45
Stainless Steel, Fine finish, 63 microinches, rms.	0.35	0.30	0.45	0.50
Stainless Steel High Polish - finish	0.20	0.25	0.30	0.30
Chrome, High Polish finish	0.10	0.10	0.20	0.35
Neoprene (50-60 Durometer.	0.70	0.70	1.40	1.10
Teflon	0.20	0.30	0.30	0.30

develops relatively lower turbulent convective heat transfer coefficient, not higher than 50 BTU/Hr-SqFt-Degree F or 0.013 BTU/Sec-SqFt-Degree F. The small zone size of the high precision stereo comparator will receive extreme high heat flux from the illuminating lamp, thus requires a large amount of cooling. The conventional air cooling process will not be applicable in this case. A sonic air jet upon impinging on film surface will develop heat transfer coefficients much higher than a conventional blower. Experience has shown that the turbulent convective heat transfer coefficients in the area of the impinging jet are comparable in magnitudes to the throat region of the sonic jet. The turbulent heat transfer coefficient can be calculated using the expression below:

$$h = \rho C_p U \frac{Nu_d}{Re_d Pr} \qquad (1)$$

Where h is the turbulent heat transfer coefficient in BTU/Sec-SqFt-Degree F. ρ is the density of air (lb/cu ft). Cp is the heat capacity of air in BTU/lb-Degree F. U is the sonic velocity in Ft/Sec. Re_d is the Reynolds number based on the diameter of the sonic throat d and Pr is the Prandtl number. Nu_d is the Nusselt number which can be related to the Re_d and Pr as follows:

$$Nu_d = 0.0243 (Re_d)^{0.8} (Pr)^{0.4} \qquad (2)$$

Introducing sonic weight flow equation

$$\dot{w} = \rho U A_T = 0.532 \frac{P_0 A_T}{T_0^{\frac{1}{2}}} \qquad (3)$$

and

$$Re_d = \frac{\rho U d}{\mu} \qquad (4)$$

where

$\dot{w}$ = Weight rate of flow (lb/sec)
A_T = Sonic throat area (ft^2)
d = Throat diameter (ft)
P_o = Cooling air supply pressure (PSF)
T_o = Cooling air temperature (Degree R)
μ = Absolute viscosity of air (Slug/ft-sec).

Substituting equations (2), (3) and (4) into (1) we have the following expression for the heat transfer coefficient, h,

$$h = 0.0243 \left(\frac{c_p}{P_r^{0.6}}\right)\left(\frac{\dot{w}}{A_T}\right)^{0.8}\left(\frac{\mu}{d}\right)^{0.2} \qquad (5)$$

For an air supply at To=560°R, h values are plotted versus P_o for various throat diameters and shown in Figure 1. h values below 0.013 BTU/Sec-Sq Ft-Degree F, are heat transfer coefficients which represent conventional air cooling.

4. HEAT BALANCE MODEL

Figure 2 shows the coordinate system of a two dimensional film heat balance model. In the present task, the scope of work involves developing a transient heat balance model for a two-dimensional film. To obtain a total film distortion pattern, it will be necessary to generate the solution using the results of the transient heat flow solution to an elastic model with friction and other mechanical loads applied to the elastic model.

4.1 TWO DIMENSIONAL TRANSIENT MODEL

The partial differential equation of a two dimensional transient heat conduction problem is well known.

FIGURE 1 SONIC AIR JET TURBULENT CONVECTIVE HEAT TRASFER COEFFICIENT

d = DIAMETER OF JET

P_o = SUPPLY AIR PRESSURE

T_o = SUPPLY AIR TEMPERATURE = 560 °R

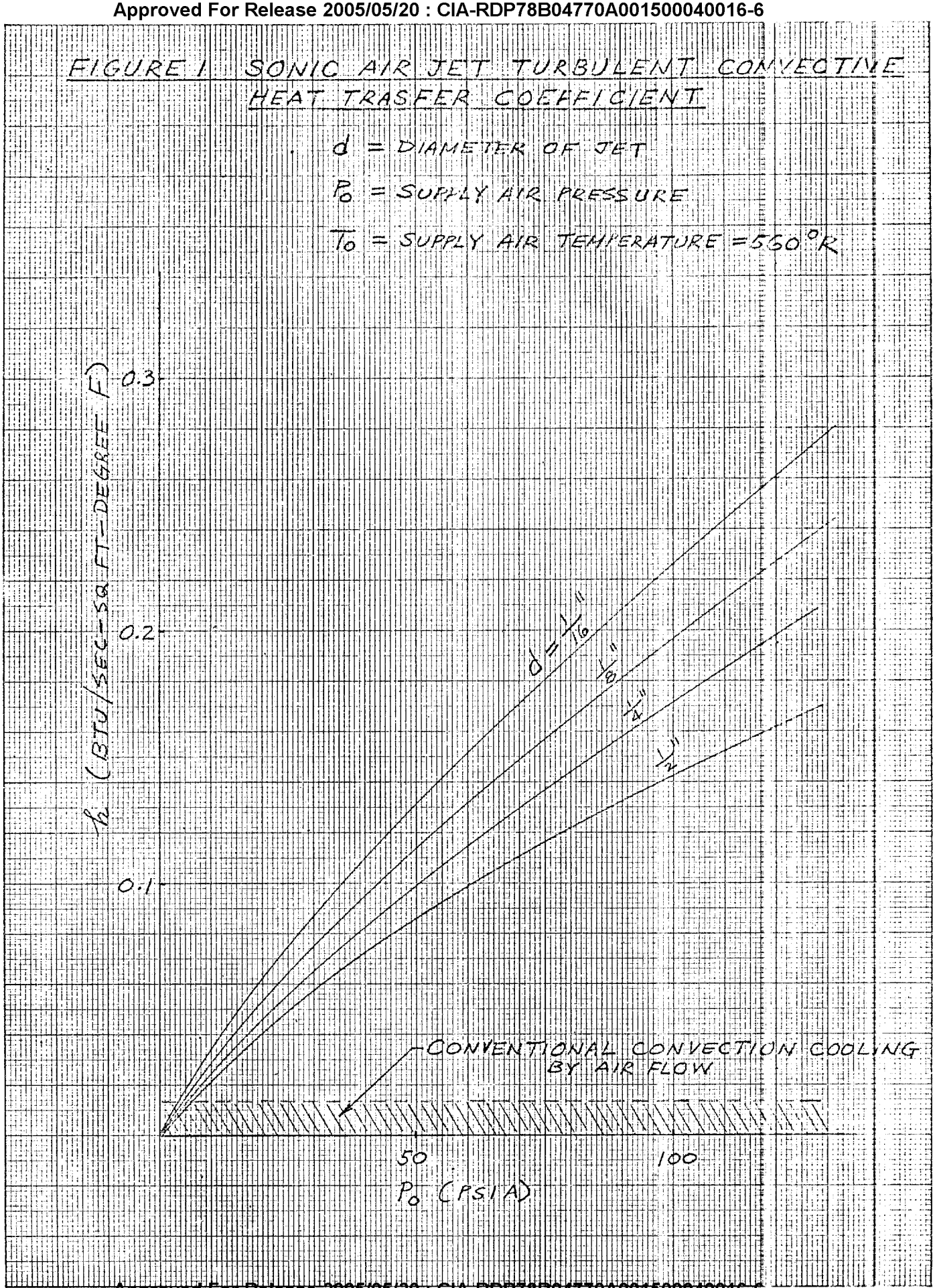

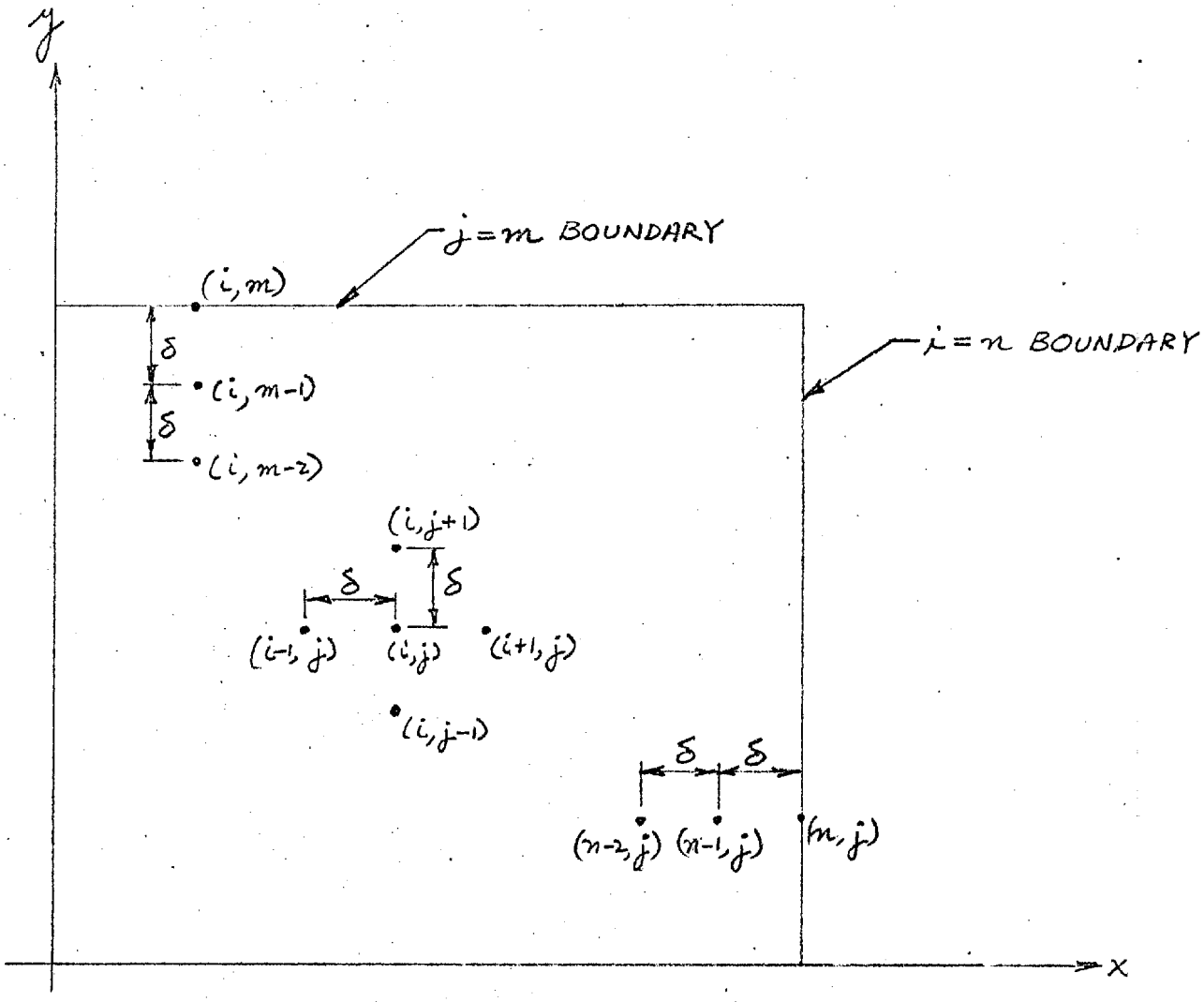

(i,j) INTERIOR POINT

(i,m) (n,j) BOUNDARY POINTS

FIGURE 2 COORDINATE SYSTEM OF TWO-DIMENSIONAL FILM

$$K\left(\frac{\partial^2 T}{\partial x^2} + \frac{\partial^2 T}{\partial y^2}\right) = \frac{\partial T}{\partial t} \tag{6}$$

K is the thermal diffusivity which equals $K_B / \rho_B C_B$. K_B is the thermal conductivity of the material, or in this case the film base (the emulsion and/or gelatin layer thickness is small as compared to the base, thus can be neglected). ρ_B and C_B are the specific weight and heat capacity of the base material. The quantities are given in section 3 of this report.

Equation (6) can be written in a non-dimensionalized form

$$\frac{\partial^2 \theta}{\partial \phi_1^2} + \frac{\partial^2 \theta}{\partial \phi_2^2} = \frac{\partial \theta}{\partial \tau} \tag{7}$$

where

$$\theta = \frac{T}{T_R}$$

$$\tau = \frac{K_B}{\rho_B C_B} \cdot \frac{t}{L^2}$$

$$\phi_1 = \frac{x}{L} \quad \text{AND} \quad \phi_2 = \frac{y}{L}$$

T_r and L are reference temperature and dimension. The reference quantities can be chosen arbitrarily.

Equation (7) is a partial differential equation. When initial and boundary conditions are specified equation (7) can be solved by numerical procedure.

For an interior point i,j (shown in Fibure 2), (7) can be written in different form

$$\left[\theta_{i,j}\right]_{\tau+\Delta\tau} = \frac{\Delta\tau}{\delta^2}\left[\theta_{i+1,j} + \theta_{i-1,j} + \theta_{i,j+1} + \theta_{i,j-1} + \left(\frac{\delta^2}{\Delta\tau} - 4\right)\theta_{i,j}\right]_{\tau} \tag{8}$$

where

$$\Delta\tau = \frac{K_B}{\rho_B C_B}\frac{\Delta t}{L^2} \qquad \Delta\phi_1 = \Delta\phi_2 = \frac{\Delta x}{L} = \frac{\Delta y}{L} = \delta$$

The initial condition of the film can be specified as the room temperature. It is reasonable to assume that the heat flux is zero along the boundary lines. Thus, the temperature for a boundary point i,m on the boundary line j=m can be calculated as follows:

$$\theta_{i,m} = \frac{4}{3}\theta_{i,m-1} - \frac{1}{3}\theta_{i,m-2} \tag{9}$$

Similarly along the boundary line i=n

$$\theta_{n,j} = \frac{4}{3}\theta_{n-1,j} - \frac{1}{3}\theta_{n-2,j} \tag{10}$$

Figure 2 shows the points described above.

When the heat flux from the illuminating source is introduced to point W on the film, transient heat flow process begins. The quantity T_w can be calculated with the differential equation below:

$$C_B \rho_B \delta_B \frac{dT_w}{dt} = h(T_0 - T_w) - \varepsilon\sigma T_w^4 + G \tag{11}$$

where

δ_B = Thickness of film base (ft)
T_0 = Temperature of the cooling jet (Degree F)
ε = Emissivity of the film surface
σ = Stefan-Poltzman radiation constant (0.48×10^{-12} BTU/(SqFt)(Sec)(Degree R)^4)
G = Heat flux from the illuminating lamp (BTU/Sec)

The solution of equation (11) can be obtained by a standard numerical procedure. The heat flux G can be estimated using the method given in Reference 6. The numerical procedure for obtaining the solution of the two dimensional transient heat flow equations discussed above is not tractable by hand calculation. It is necessary to program the solution for a high speed digital computer. The solution will yield temperature-time histories of a grid of points on the two dimensional film. The dimensional changes of the film with time can then be calculated using the temperature solution as input.

4.2 ONE DIMENSIONAL STEADY STATE MODEL

It is of interest to investigate the local distortion of film in the area of illumination. Considering the heat balance is at steady state condition the left hand side of Equation (11) is zero. In addition, the radiative heat rejection $\varepsilon \sigma T_w^4$ is usually negligible. Therefore the one dimensional steady state heat balance will be

$$h (T_0 - T_w) = G = h \Delta T \qquad (12)$$

Figure 3 shows the relation of h, G and ΔT. In the next section, numerical examples are given to estimate the local distortion of film subjected to high intensity light of the high precision stereo comparator.

5. NUMERICAL EXAMPLES

Preliminary design data of the high precision stereo comparator indicate that the power of the illuminating lamp will be 500 KW and the illuminated zone area at the film gate is between 0.030 to 0.75 square inch. The radiated power absorbed by the film at the film gate for the 500 KW xenon lamp is estimated to be 8 watts, based on the data given in Reference 6.

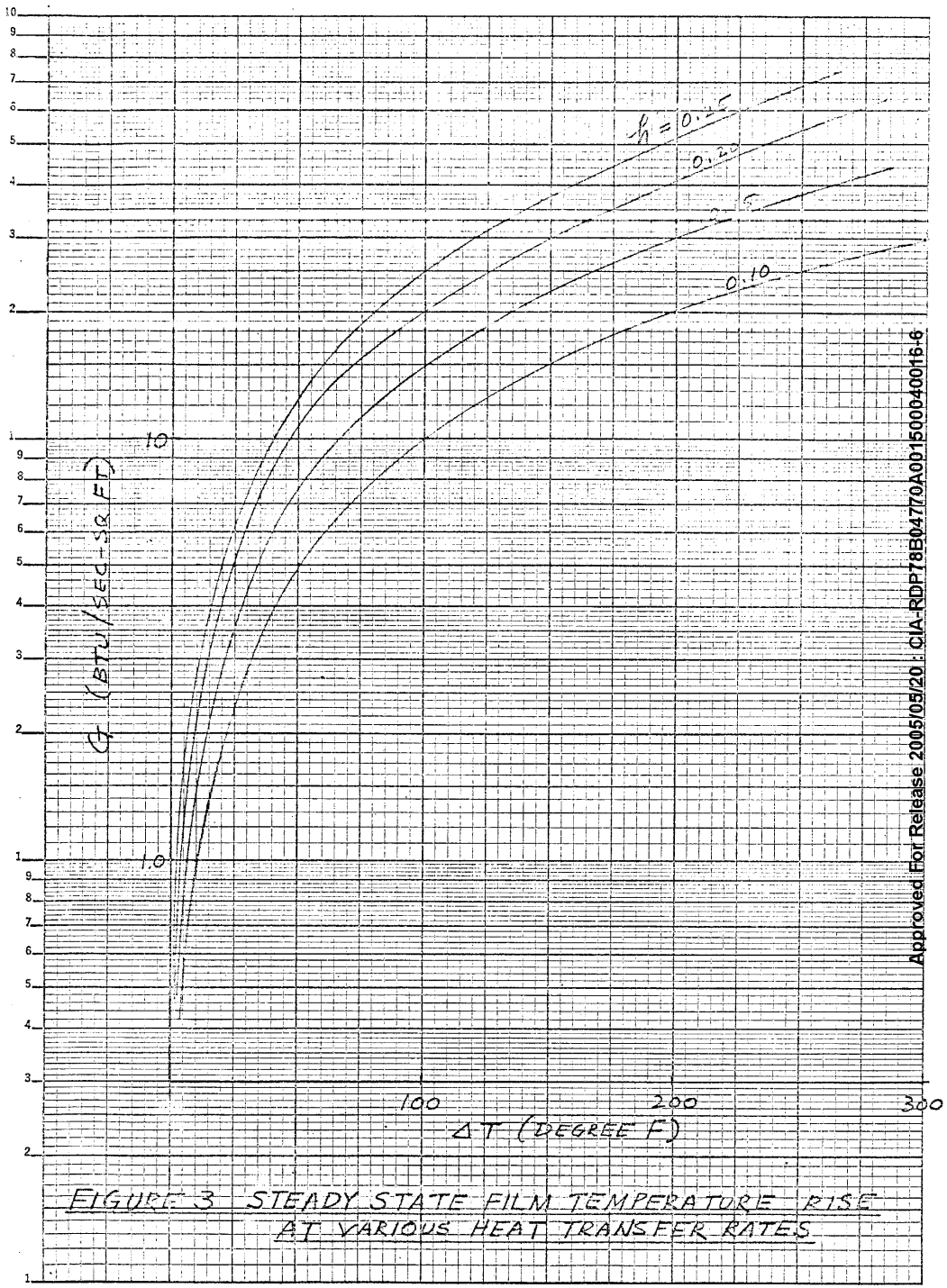

FIGURE 3 STEADY STATE FILM TEMPERATURE RISE AT VARIOUS HEAT TRANSFER RATES

Let the illuminated zone area be A, then the radiation flux density, G, will be:

$$G = \frac{8 \text{ watts}}{A} = \frac{.755 \times 10^{-2}}{A} \quad \frac{BTU}{Sec\text{-}SqFt}$$

5.1 CASE 1 SMALLEST ILLUMINATED AREA

For $A = 0.030$ in^2 then $G = \frac{.755(1.44)}{.03} = 32.6 \frac{BTU}{Sec\text{-}SqFt}$

For conventional air cooling the best obtainable heat transfer coefficient is $h = 0.013$ and the temperature rise will be 2.5×10^3 which is unacceptable. For a sonic jet, assume $T_o = 60^oF$, $P_o = 60$ PSI and the cooling jet diameter be $d = \frac{1}{16}$ " .

The h value can be obtained from curves on Figure 2.

$$h = 0.152 \frac{BTU}{SEC\text{-}ft^2\text{-}Deg\ F}$$

ΔT value can be obtained from Figure 3.

$$\Delta T = 215^o\ F$$

If the initial film temperature is 60^o, the final temperature will be 275^o F which will not ignite the film but is still unacceptable. The radius of $A = 0.030$ in^2 is approximately .05". The thermal expansion of the radius is

$$\epsilon \text{ Estar} = 0.04" \times 0.0001 \times 215 = 0.0001075"$$
$$= 0.274 \times 10^{-6} \text{meter}$$
$$\epsilon \text{Triacetate} = 0.005" \times 0.0003 \times 215 = 0.722 \times 10^{-6} \text{meter}$$

5.2 CASE 2 LARGEST ILLUMINATED AREA

For $A = 0.75\ in^2$, $G = 1.45\ \frac{BTU}{Sec\text{-}SqFt}$

For conventional cooling, again the best obtainable heat transfer coefficient is 0.013. The temperature rise will be 111^oF and the dimensional changeacross the illuminated area would be 0.42 millimeters. For Sonic Jet Cooling:

Let $T = 60^oF$ $P_o = 60$ PSI and $d = \frac{1}{2}"$

From Figure 2 $h = .1\ \frac{BTU_2}{Sec\text{-}Ft^2\text{-}Deg.F}$

From Figure 3 $T = 14.5^oF$

The radius of $A = .75\ in^2$ is approximately .50 in.

The growth of the radius is

$\in Estar = .50" \times .0001 \times 14.5 = .000725$

or $= .185 \times 10^{-6}$ meter which is acceptable.

The cases above are numerical examples to show the magnitudes of local film distortion due to thermal expansion. We must point out that use of sonic jet cooling is highly undesirable. The jet screams producing a very high local noise level and momentum force of the jet produces vibration in the platen and measuring engine structure.

REFERENCES

1. "Manual of Physical Properties of Kodak Aerial and Special Sensitized Materials", Eastmen Kodak Company, Rochester, N. Y., May, 1965.

2. Calhoun, J. M.; "The Physical Properties and Dimensional Stability of Safety Aerographic Film", Photogrammetric Engineering, 13, pp 163-221, June, 1947.

3. Calhoun, J. M., and Leister, D. A.; "Effect of Gelatin Layers on the Dimensional Stability of Photographic Film', Photographic Science and Engineering, 3: 8-17, February, 1959.

4. "Physical Properties of Kodak Estar Base Films for the Graphic Arts", Eastman Kodak Company, Rochester, N. Y., 1966.

5. Eckert, E. R. G., and Drake, R. M; "Heat and Mass Transfer", McGraw-Hill Book Company, Inc., 1959.

STAT

515078

STAT

Task 2
Contribution of Stereo

Research Effort in Support of
High Precision Stereo Comparator

Approved For Release 2005/05/20 : CIA-RDP78B04770A001500040016-6

STAT

September 5, 1967

Mailing Address

STAT

RESEARCH EFFORT IN SUPPORT OF
HIGH PRECISION STEREO COMPARATOR

Task 2 the Contribution of Stereo

Work Statement: There is considerable qualitative evidence that stereo improves measuring accuracy. In addition, there is a vast body of documentation on stereo. This literature will be reviewed and the data extracted which is pertinent to the precision comparator criteria. An attempt will be made to establish quantitative evidence for the contribution of stereo to measuring accuracy.

Submitted by

STAT

STAT

September 5, 1967

RESEARCH EFFORT IN SUPPORT OF HIGH PRECISION STEREO COMPARATOR

Task 2 the Contribution of Stereo

Contents

List of Tables

1. Summary and Conclusions

In the literature review, no quantitative evidence was found to substantiate a contribution of stereo to measuring accuracy. In fact, the only quantitative evidence available indicated that stereo degraded measuring accuracy. In addition, parallax clearance studies suggest that the qualitative evidence that stereo improves measuring accuracy may be illusory.

Investigations into photogrammetric errors by Zeiss in Oberkochen, Germany, indicated that operator point setting accuracy was significantly better in monoscopic viewing than in stereoscopic viewing. Thus the question immediately arises as to why should a precision comparator incorporate stereoscopic viewing if point setting in monoscopic viewing is more accurate? The question becomes trivial with respect to the High Precision Stereo Comparator since it must be used to measure heights, volumes and grades and the stereo capability is essential.

The question is not trivial however with respect to design features of the comparator. Thus, monoscopic viewing of each stage separately becomes an important feature and it is well that it is to be incorporated into the High Precision Stereo Comparator.

A study by Karara at the University of Illinois appeared at first to contradict the findings of Zeiss. A closer examination of the test conditions, however, indicated that there was no contradiction and in fact, the study did not provide a true basis for comparing monoscopic and stereoscopic point setting accuracy. There is a serious question regarding utilization of the data reported. It was not apparent that the test procedures provided good control of the variables affecting operator point setting accuracy. In spite of this, however, the indication that a truly significant improvement in measuring accuracy may be obtained by revising operator techniques should not be overlooked.

We conclude therefore, that monoscopic and stereoscopic point setting accuracy should be measured under controlled conditions and that operator techniques be devised and tested under controlled conditions for maximizing measuring accuracy.

2. Ahrends Report of Zeiss Data

In 1964 at the International Conference of Photogrammetry at Lisbon, Portugal, an "Analysis of Photogrammetric Errors" was reported by Martin Ahrend of the Zeiss works, Oberkochen (Ref.1). The analysis was a comprehensive separation of errors encountered in the photogrammetric process. The data came from long range investigations by the Photogrammetric Laboratory at the Zeiss works.

Errors from the following sources were reported:

Camera Lens (130 Aerial Survey Cameras)
Pressure Plate unevenness
Film (both acetate and polyester)
Printing (on plates)
Comparator (Zeiss PSK)
Analog Plotter (C-8 Stereoplanigraph)
Point setting (Mono)
Point setting (Stereo)
Point setting (Stereo transfer) .

For the present effort, we were interested in the results of point setting (Mono) and point setting (Stereo) which were contrary to the experienced opinion of many photogrammetrists. The reported data was the "Point Setting Mean Square Coordinate Error", at the image plane, see Table I. Approximately 1600 settings were made by 3 operators. The focal length was 153 mm and the altitude was 1500 meters. Viewing magnification varied from 1 to 200.

The startling conclusion is that the test data indicate that point setting by monoscopic viewing is considerably more accurate than point setting by stereoscopic viewing. It is particulary strange since the stereoscopic acuity of depth discrimination is reportedly 30 times better (2 seconds of arc) than monoscopic acuity, (1 minute of arc) (Ref. 2, p. 392).

TABLE I

ZEISS MEASUREMENTS OF POINT SETTING ERROR

MEAN SQUARE COORDINATE ERROR, MICRONS

Image Area	92mmx184mm			184mmx184mm		
Focal Length	15cm	30cm	60cm	15cm	30cm	60cm
MONO White Boundary Points or similar natural Points.	±1.6	±1.6	±1.6*	±1.6	±1.6	±1.6
STEREO White Boundary Points in y-direction	±3.3	±3.3	±3.3	±3.3	±3.3	±3.3
STEREO White Boundary Points x-direction	±2.9	±2.9	±2.9	±2.9	±2.9	±2.9

1600 settings by 3 operators, magnifications from 1 to 200.

* Viewing magnification 16

3. Literature Survey

A literature survey was undertaken to determine whether other investigations had been made which would support or refute the results reported by Ahrends. Basically three areas of the technical literature were searched, (see Bibliography).

a.) Psychological research into stereoscopic vision.

b.) Journals of the Photographic Societies: SMPTE, SPIE, SPSE.

c.) Journal of the Society of Photogrammetry "Photogrammetric Engineering".

No reports were found in any of this literature relating to a comparison of point setting accuracy for monoscopic and stereoscopic viewing.

However, in a bibliography on "Stereo-Mensuration" provided by Boeing Aircraft Company, mention was made of work being done under Army Contract by Dr. H. M. Karara at the University of Illinois. This was the only work on the subject which we could discover.

4. Karara's Report of University of Illinois Data

Dr. H. M. Karara, Professor of Civil Engineering at the Surveying and Photogrammetry Department of the University of Illinois, Urbana, Illinois, is conducting a study for the U.S. Army Engineers, Ft. Belvoir.

A report of their first years work was published in February 1967 by the University (See Ref.4).

The study to date is principally concerned with the comparison of the precision of point transfer in the monocular and the stereoscopic approaches in analytical photogrammetry. Dr. Karara's group used large scale photography, 1:5700, of Urbana flown for them by Chicago Aerial Survey. Measurements were made with the WILD STK-1 Stereocomparator at 20x magnification. The report was concerned exclusively with the accuracy of point transfer. Although the report stated that the results indicated that the stereoscopic approach was significantly more precise than the monocular approach, they

also concluded that the difference was mainly due to the point marking system in the point transfer device used. In spite of the emphasis of the work on point transfer it appears to be possible to extract some conclusions regarding the precision of pointing, (see Table II). The data is not conclusive but it appears to favor stereo slightly. For both stereo and mono measurements, the image points were premarked by drilled holes. Coordinates were measured by centering the measuring marks on the drilled holes, not on the imagery.

5. Discussion of Point Setting Accuracy

It appears that depth discrimination in stereo viewing is not utilized in point setting. In fact, it is possible that residual parallax error encountered in stereo viewing could be added to point setting error. If that were so, then the Zeiss data would be comprehensible since an operator probably would not be aware of the residual parallax clearance.

The magnitude of the residual parallax clearance is significant. The international training Center (ITC) at Delft, the Netherlands, measured the residual parallax clearance for a number of conditions, (Ref.3). The parallax clearance capability is affected by the parallax in the orthogonal direction, image resolution, magnification and measuring mark size. Under the best conditions, however, the standard deviation of parallax clearance is no better than 2½ to 3½ microns, (Ref.3, p. 13). Why then did the University of Illinois study not show a significant difference in pointing error for the monocular and stereoscopic approach. Perhaps the residual parallax clearance phenomena was not operating in their tests. In preparation for viewing in stereo, the points to be measured were marked by a drilled hole in one plate only. "After the y-parallax is removed in the vicinity of the point, the measuring mark is then centered in the single drilled hole which appears super-imposed on the terrain image". (See Ref.4, p. 1). Thus it appears that in the stereo portion of the test, the point setting was actually done monocularly and not stereoscopically. The point transfer aspects

TABLE II

UNIVERSITY OF ILLINOIS MEASUREMENTS

OF POINT SETTING ERROR

STANDARD DEVIATION, MICRONS

(6 measurements of each image point and fiducial mark by one operator)

	Average Std. Dev. of 50 Image Points	Average Std. Dev. of 4 Fiducial Marks
MONO		
x-coordinate	2.2	0.8
	2.3	0.8
y-coordinate	2.4	0.8
	2.5	0.8
STEREO		
x-coordinate	1.9	0.7
y-coordinate	2.5	0.8

of the University of Illinois study are not pertinent to our conclusions. Thus, in our opinion, the Zeiss data are not refuted by the University of Illinois data.

The implications are significant with respect to the precision stereo comparator. We recommend that a study be conducted to determine the procedures and conditions which will minimize operator point setting error.

If, as implied by the Zeiss data, the operator point setting accuracy can be improved by a factor of 2 or more, that would indeed be a significant improvement.

REFERENCES

1. Ahrend, M.; "Analysis of Photogrammetric Errors", Carl Zeiss, Oberkochen, Germany, 1966, pp 62-78.

2. Palmer, D. A.' "Steroscopy and Photogrammetry", Photogrammetric Engineering, Vol , pp 391-394.

3. Research by the International Training Center ITC at Delft., the Netherlands for Itek Corporation, Lexington, Conn., Report of Program 9221-P.D.-1, period: February-July 1966.

4. Karara, Dr. H. M.; "Mono Versus Stereo Analytical Photogrammetry", University of Illinois, Urbana, Illinois, February 1967.

BIBLIOGRAPHY

a.) Psychological Research into Stereoscopic Vision.

1. Julesz, B.; "Stereopsis and Binocular Rivalry of Contours", J. Opt. Soc. Amer., Vol. 53, pp 994-999, August 1963.

2. Julesz, B.; "Texture and Visual Perception", Scientific American, Vol. 212, pp. 38-48, Feb. 1965.

3. Kaufman, L.; "On the Spread of Suppression and Binocular Rivalry",Vision Research, Vol. 3, pp.401-415, 1963.

4. Kaufman, L.; "Suppression and Fusion in Viewing Complex Stereograms", American J. of Psychology, Vol. 77, pp. 193-205, 1964.

5. Kaufman, L.; "On the Nature of Binocular Disparity", Amer. J. of Psychology, Vol. 77, pp. 393-402, Sept. 1964.

6. Kaufman, L.; " Some New Stereoscopic Phenomena and Their Implications for the Theory of Steropsis", Amer. J. of Psychology, Vol. 78, pp. 1-20, March 1965.

7. Kaufman, L.; "Further Observations on the Nature of Effective Binocular Disparities", Amer. J. of Psychology, Vol. 78, pp 379-391, September 1965.

8. Davson, Hugh; "The Eye: Volume 4, Visual Optics and Optical Space Sense", Academic Press, 1962.

9. Graham, Clarence H.; "Vision and Visual Perception", John Wiley & Sons.

10. O'Conner, D.; "Possible subjective Edge-Adjacency Effects in Photogrammetric Coordinate Measurement", Seminar Proceedings'The Human in the Photo-Optical System, New York, April 1966.

b.) Journals of the Photographic Societies: Society of Motion Picture and Television Engineers, (SMPTE); Society of Photographic Instrumentation Engineers, (SPIE); Society of Photographic Scientists and Engineers, (SPSE).

No reports were found for the past 10 years regarding the subject.

c.) Photogrammetric Engineering

1. Hothmer, J.; "A Test of the Nistri Photostereograph Model Beta Instrument", Photogrammetric Engineering, Vol. 26, pp 720-725, December 1960.

2. Lyon, D.; "Let's Optimize Stereo Plotting", Photogrammetric Engineering, Vol. 30, pp 897-911, November 1964.

3. Miller, C. I.; "The Stereoscopic Space Image" Photogrammetric Engineering, Vol. 24, pp 810-815, December 1958.

4. Miller, C. I.; "Vertical Exaggeration in the Stereo Space-Image and Its Use", Photogrammetric Engineering, Vol. 26, pp 815-818, 1960.

5. Moesner, K. E.; "Comparative Usefulness of Three Parallax Measuring Instruments in the Measurement and Interpretation of Forest Stands", Photogrammetric Engineering, Vol. 27, pp 705-709, December 1961.

6. Pryor, W. T.; "Relationship of Topographic Relief, Flight, Height, and Minimum and Maximum Overlap", Photogrammetric Engineering, Vol. 25, pp 572-589, September 1959.

7. Skidmore, J. R.; "Contour Accuracy Vs. Spot Heights", Photogrammetric Engineering, Vol. 31, pp 828-830, September 1965.

8. Stanton, J. W.; "The Wild A-7 Autograph as a Comparator", Photogrammetric Engineering, Vol. 28, pp 455-461, 1962.

9. Veres, S. A.; "The Effect of the Fixation Disparity on Photogrammetric Processes", Photogrammetric Engineering, Vol. 30, pp 148-153, January 1964.

10. Johnson; "Stereo Perception Limit", Photogrammetric Engineering, Vol 23, pp 933, 1957.

11. Hallert; "Error of a Standard Observation", Photogrammetric Engineering, Vol. 23, p 179, 1957.

12. Mahoney; "Measuring Accuracy and its Relation to Model Deformations and Other Measurements Made in a Stereo Model", Photogrammetric Engineering, Vol. 22, p 764, 1956.

d.) Other Sources

1. Ahrend, M.; "Analysis of Photogrammetric Errors", Carl Zeiss, Oberkochen, Germany, 1966, pp 62-78.

2. Ogle, K. N.; "Precision and Validity of Stereoscopic Depth Preception from Double Images", J. Opt. Soc. Amer., Vol. 43, pp 906-913, October 1953.

3. U. S. Army Contract CN DA-44-009-AMC-133, "Study of Mono Versus Stereo Analytical Photogrammetry", Univ. of Illinois; Dr. H. M. Karara -- Principal Investigator.

S 150858

STAT

TASK 4

Calibration

Research Effort in Support of
High Precision Stereo Comparator

STAT

[redacted]

November 3, 1967

Mailing Address

STAT

[redacted]

RESEARCH EFFORT IN SUPPORT OF
HIGH PRECISION STEREO COMPARATOR

Task 4 Calibration

Work Statement: Ready and reliable calibration of the precision comparator to a separate objective standard is desired. It may be impractical that a machine be considered to be completely self-checking and self-policing. Most desirable, of course, is that determination of measurement accuracy be traceable directly to the Bureau of Standards' standards of length.

We will examine the feasibility and make an analysis of the errors of calibration to recommend a course of action.

Submitted by:

[redacted]

STAT

STAT

[redacted] November 3, 1967

RESEARCH EFFORT IN SUPPORT OF HIGH PRECISION STEREO COMPARATOR

Task 4 Calibration

Contents

STAT [redacted] November 3 1967

List of Figures

Approved For Release 2005/05/20 : CIA-RDP78B04770A001500040016-6

Summary and Conclusions

Measuring errors of a precision comparator are associated with many factors: The accuracy of the measuring element; straightness, looseness and orthogonality of the ways; tilt of the ways and optical axis; structural drift due to relaxation; thermal distortions; film non-uniformities and operator point setting error. Calibration of a precision comparator should detect all the errors and the accuracy and precision of the calibration device should be better than that of the comparator. (See Appendix A for definition of accuracy and precision.) For these reasons, it it not considered practical for a machine to be self-calibrating. We are concerned with two-dimensional measurements. The scope of this report does not include errors associated with the stereo-process.

Two techniques for calibration have been considered:

a.) Direct, independent measurement of the comparator platen travel and a comparison of the comparator readings to the measured travel.

b.) Use of the comparator to measure a scale which has been calibrated by the Bureau of Standards and a comparison of the comparator readings with the calibrated values.

The strength of the first method is in its superlative precision. By special techniques, a laser interferometer can readily measure platen travel to a precision of .01 microns or better. The weakness of the first method is that it does not include all the error sources. In fact it only measures the accuracy of the measuring element and in the high precision stereo comparator that is likely to be the smallest component of the total error. For this reason, the first method is not recommended.

The strength of the second method is that it does include nearly all the error sources. ("Nearly" will be discussed later.) In addition, laying a transparent scale on the platen of the comparator is quick and easy, and does not change or require moving the machine. Calibration of the scale can be directly traceable to the Bureau of Standards' standards of length.

A difficulty which must be overcome is the operator point setting accuracy. The technical literature indicates that the error involved in having an operator set a measuring mark in the comparator microscope in coincidence with an image mark is on the order of $\pm$ 1 micron, rms. Errors of such magnitude would completely mask the calibration and are unacceptable. A proven technique for obtaining high precision and repeatability in centering a microscope on a scale mark is that used by the Bureau of Standards in

in calibrating scales. By using a variation of the Bureau of Standards' equipment, we will operate on the image of the scale mark which is formed by the comparator microscope. All the errors associated with the microscope will thus be included. Point setting precision can be improved by a factor of 20 or more. The Bureau of Standards achieves point setting precision to a standard deviation of about $\pm$ .05 microns. In measuring a standard meter bar, the Bureau of Standards obtained an accuracy of $\pm$ 0.035 micron. Such accuracy in a calibration device would be entirely satisfactory. While there is no way to guarrantee that such accuracy can be obtained, it seems reasonable to expect it. There is one obvious limitation to using a scale on glass or other transparent substrate. The thickness of the scale (¼-inch or more) prevents using it with the highest magnification of some microscopes because the clearance between the comparator platen and the microscope objective and the focussing range of the microscope is too small. In such cases a lower power objective must be used for calibration.

The Bureau of Standards cannot calibrate a two-dimensional grid to our required accuracy, therefore a linear scale must be used. With a linear scale the x- and y- coordinates of a comparator can be independently calibrated by laying the scale parallel to the coordinate axis. The

coordinates can be jointly calibrated by laying the scale at some angle such as 45 degrees to the axes.

We previously stated that "nearly" all error sources are included in a calibration by the second method. The method deliberately excludes errors associated with the properties of the film and operator point setting errors. Such errors have sources other than the instrument being calibrated and could easily mask the calibration. Once a machine calibration is made however, an investigative program could be established to determine the measuring errors associated with the properties of photographic film and the operator point setting errors for that particular machine.

We conclude that it is entirely feasible to make a calibration device for the ready, reliable calibration of the High Precision Stereo Comparator. The device could also be used to calibrate other precision comparators.

We recommend the following course of action:

(a.) Design and make a suitable scale on a transparent substrate such as quartz or Cer Vit.

(b.) Have the U. S. Bureau of Standards calibrate the scale to the best available accuracy.

(c.) Design and make an electronic point setting device.

(d.) Calibrate several existing precision comparators

(e.) Recommend revisions (if any) for the calibration of the Hight Precision Stereo Comparator.

1. Machine Errors

The broad class of errors involved in the mensuration task in analytical photogrammetry can be separated into several catagories:

(a.) Built in accuracy of machine components

(b.) Dimensional changes caused by environmental changes.

(c.) Usage.

We are concerned here with two-dimensional measurements made on photographic film by means of a precision comparator. The scope of this report does not include errors of registration between the two platens of a stereo comparator or other errors uniquely associated with the stereo process.

Sources of residual error due to the built in accuracy of machine components are:

(a.) Precision of the measuring element.

(b.) Bias of the measuring element.

(c.) Straighness of the ways.

(d.) Looseness in the bearings.

(e.) Orthoganality of the ways.

(f.) Location of the measuring element relative to the film plane.

(g.) Tilt variation of the microscope axis with respect to the measuring element.

(h.) Tilt variation of the ways with respect to the measuring element.

(i.) Tilt variation of the film plane with respect to the measuring element.

(j.) Drift due to relaxation of stresses locked into structural materials.

The sources of error caused by dimensional change due to the environment are:

(a.) Change of the measuring element.

(b.) Distortion of ways.

(c.) Dimensional change of the platen.

(d.) Distortion of the structure which changes the relation of the microscope optical axis, film platen and measuring element.

The sources of error attributable to usage are:

(a.) Operator point setting errors.

(b.) Film distortion due to non-uniform flattening on the platen.

(c.) Film distortion due to thermal and/or humidity inputs of the comparator and its environment.

2. Objectives of Calibration

It is highly desirable that a calibration device have several attributes which should be better than the equipment to be calibrated:

(a.) Precision should be finer than the machine being measured.

(b.) Bias, if any, should not change.

(c.) All errors in the measuring process should be detected by the calibration device.

(d.) Calibration of the calibration device should be directly traceable to the Bureau of Standards' standards of length.

(e.) The calibration device should not be affected by environmental changes.

For the above reasons, it appears that we should not depend on a precision comparator to be self calibrating.

The utility of a calibration device depends upon several things:

(a.) The comparator should remain in its normal operating environment during calibration.

(b.) The comparator should not be modified for calibration in a way which may change the measuring accuracy.

(c.) The measuring procedure should not be modified for calibration in a way which may change the measuring accuracy.

(d.) The calibration device should be subject to the same vibration environment as the platen, microscope and measuring element of the comparator.

(e.) The calibration device set up procedure should be simple and calibration should not require excessive time.

(f.) One calibration device should be suitable for calibrating a number of different comparators.

Several of the above come under the heading of minimum down time. It is often during periods

of heavy usage that the accuracy of a comparator becomes suspect and the need for calibration is urgent. The machine cannot be spared for long and therefore calibration to be useful must be quick and easy. Also, if calibration is quick and easy, a regular schedule of calibration checks can be set up which would be acceptable to the operating groups.

Two techinques for calibrating comparators have been considered and each will be discussed in the following sections. The two techniques are:

(a.) Direct, independent measurement of the comparator platen travel and a comparison of the comparator readings to the measured travel.

(b.) Use of the comparator to measure a scale which has been calibrated by the Bureau of Standards and a comparison of the comparator readings with the calibrated values.

3. Direct Measure of Platen Travel

The laser interferometer offers a high precision capability for direct measure of platen travel. By suitable arrangement of mirrors, both axes can be measured. For a helium-neon gas laser, the wavelength of the laser light is 0.6328 microns. An interference fringe appears every half wavelength, therefore, the least count of fringes is 0.3164 microns. By suitable null-balance techniques, a fringe can easily be divided into almost as many parts as desired. It is entirely possible to detect 1/30 fringe and obtain a least count

of 0.01 microns.

There are two environmental inputs which can affect the accuracy of the least count: the wavelength drift of the laser and the affect of atmospheric changes on the wavelength. The following values obtained from the Bureau of Standards were reported in Reference 1, Page 31:

(a.) Air Temperature Correction
-0.928 parts per million/^{o}C

(b.) Barometric Pressure Correction
+0.357 parts per million/mm Hg

(c.) Humidity Correction
-0.057 parts per million/mm Hg

(d.) Wave length drift measurement limited by measuring accuracy. Less than .03 parts per million.

For measurement of large dimensions, on the order of 1/10 meter or more, the laser interferometer reading would require corrections. For measurement of small dimensions, on the order of 1 cm or less, the reading error would be:

(a.) $\mp$ 0.00928 microns/^{o}C

(b.) $\pm$ 0.00357 microns/mm Hg

(c.) $\pm$ 0.0003 microns drift

which is negligible unless large changes in the environment occur. Thus the least count and the accuracy of a laser interferometer are excellent and probably well beyond that required for calibration of a precision comparator.

The disadvantage of the laser interferometer

is that it does not detect all the errors in the measuring process. It will not detect errors in straightness, orthogonality or tilt of the ways. It will not detect any errors associated with the microscope. The High Precision Stereo Comparator itself will use a laser interferometer as the measuring element. If properly designed, the comparator measuring element should be equally as good as the calibrator measuring element. For these reasons, we do not recommend that a laser interferometer be used as a calibration device.

4. Calibrated Optical Scale

Gage blocks, calibrated by the Bureau of Standards, are the classical approach to determining the accuracy of devices for linear measure. They fulfill all of the objectives mentioned in section 2. While gage blocks themselves cannot be used on a stereo comparator, a calibrated optical scale, such as shown in Fig. 1, can. The procedural principals are the same.

While the exact design of the scale is not critical, there are some aspects which require critical examination in order to be certain that the machine calibration requirements will be satisfactorily fulfilled. First, however, note that placing the calibrated scale on the platen of a comparator is quick and easy. Measuring the spacing of the graduations does not change the normal measuring procedure and errors of straightness, orthoganality and tilt of the ways

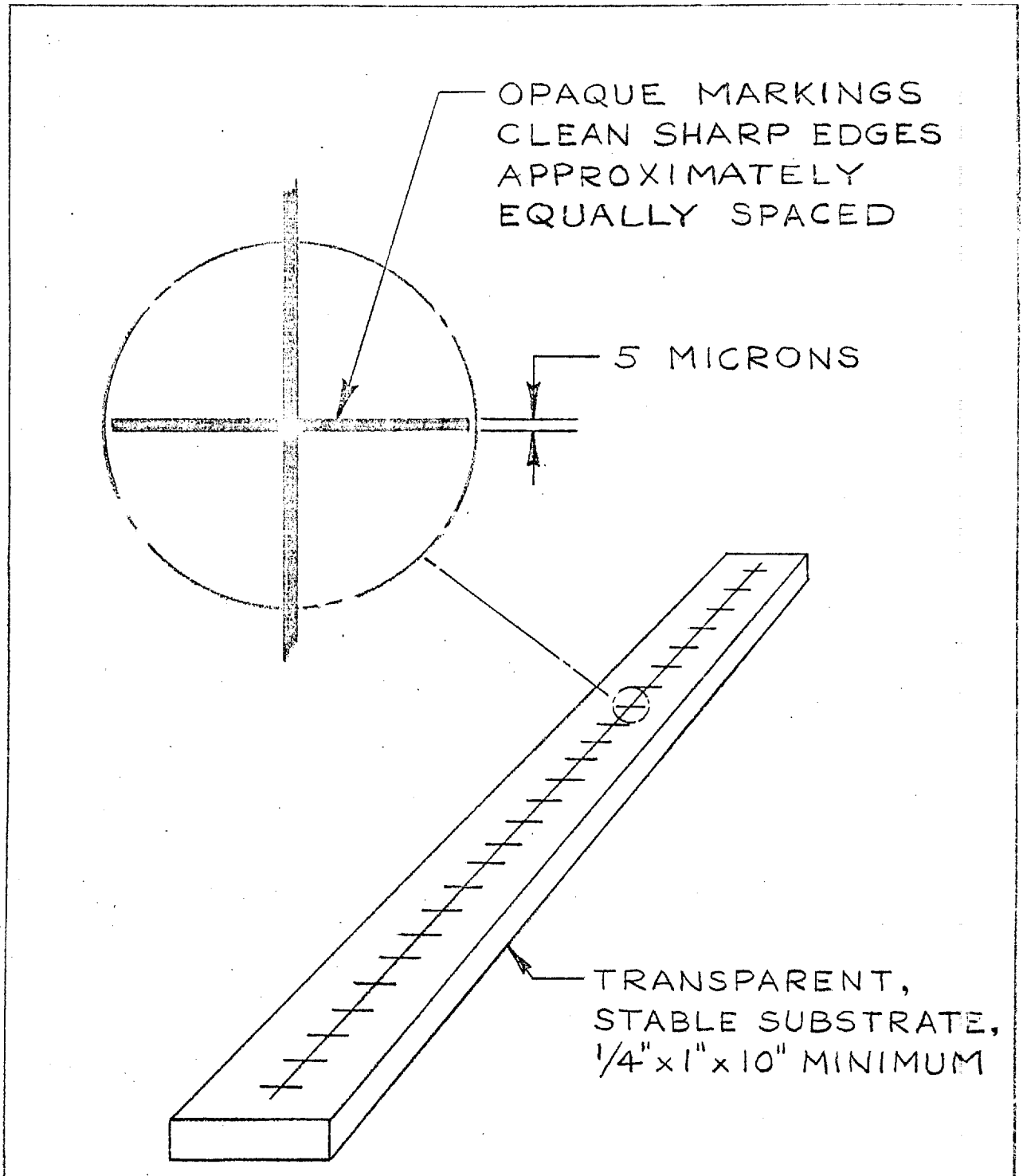

FIG. 1 CALIBRATED OPTICAL SCALE

will be detected. Errors associated with the microscope will be detected.

The Bureau of Standards cannot calibrate a two-dimensional grid to our required accuracy therefore a linear scale must be used. A linear scale however, is versatile and fully as satisfactory as a two-dimensional grid. The x- and y- coordinates of a comparator can be independently calibrated by laying the scale parallel to the coordinate axis. The error, e_L , in measuring a calibrated length is:

$$e_L = e_x \cos \theta + e_y \sin \theta$$

where: θ = Angle of the calibrated length to the x-axis.

e_x = Error in measuring the x-coordinate length.

e_y = Error in measuring the y-coordinate length.

If in calibrating the x-axis we wish the error contribution of the y-axis to the total error to be 5% or less of the x-axis error, the scale must be parallel to the x-axis within $\pm$ 3 degrees. Such alignment accuracies may be easily achieved.

The x- and y- axes can be jointly calibrated by laying the scale at an angle to the axes. The error contribution of each axis will have equal weight if the calibrated scale is at 45 degrees to the comparator axes. Errors in straightness and orthogonality of the ways can thus be detected.

Aspects which require critical examination are:

(a.) Calibration of the scale.
(b.) Change of the scale with temperature.
(c.) Operator point setting accuracy.

The Bureau of Standards can calibrate the markings on a linear scale and certify the calibration to ± 1/4 micron on a special order if the markings are of suitable size and clarity. Although ± 1/4 micron may be sufficiently accurate for large measurements, 10 cm or more, we would prefer better accuracy for small measurements, 1 cm or less. By requesting the Bureau of Standards to make a multiplicity of readings on each mark, with the readings spread over several days and with the scale turned end for end several times, we will obtain a statistical set of calibration readings. From this set we can obtain random error and bias error. From a statistical analysis we can assign values to the measured intervals which we can probably depend upon to be considerably more accurate than ± 1/4 micron. When the Bureau of Standards used their calibration equipment to measure the length of a standard meter bar, (reference 2), agreement with the assigned length was obtained to 7 parts per 100 million. This accuracy is equal to ± 0.035 microns over a 1 meter length. Such accuracy would be entirely satisfactory.

Change of the scale length after calibration and during use must be avoided or corrected. For a glass-type substrate, thermal inputs are the

principal sources for change in length. Thermal coefficients of linear expansion of the various glasses are:

Selected flat plate glass	10.8	parts per million/°C
BSC Optical flat	9.0	"
Pyrex	3.6	"
Ohara Low Expansion glass	2.4	"
Quartz, fused	0.5	"
Owens-Illinois Cer-Vit Crystalline glass	0.0	"

We would prefer the substrate dimensions be insensitive to temperature change (over a reasonable temperature range such as $\pm$ 5°C), since it is often difficult to know exactly what the temperature of the substrate is at the time of measurement. For a 25 cm (10-inch) length, the dimensional change would be:

	Temperature 10°C	Change 2°C
Selected flat plate glass..	27 microns	5.2 microns
BSC Optical flat	22.5 "	4.5 "
Pyrex	9 "	1.8 "
Ohara Low Expansion Glass..	6 "	2.4 "
Quartz, fused	1¼ "	¼ "
Owens-Illinois Cer-Vit Crystalline glass	0.0 "	0.0 "

Quartz would probably be a satisfactory substrate for temperature variations up to 2°C for measurements of 10 cm or more. For measurements of 1 cm or less,

quartz would be entirely satisfactory. The magnitude of the necessary correction is illustrated in Fig. 2.

To insure that the scale markings would not move with respect to the substrate, a filled scratch or metal deposited markings would be desirable. Markings carried in an emulsion on the surface of the substrate would probably be undesirable.

Since a transparent substrate will be at least ¼-inch thick, there may be some difficulty in using it on some comparators with very high power microscopes. The clearance between the comparator platen and the high power microscope objective may be less than ¼-inch. The focus range of most instruments will generally accommodate more than ¼-inch. If on certain instruments it does not, then a lower power objective must be used for the calibration.

5. Operator Point Setting

A major item of uncertainty in using an optical scale for calibrating a precision comparator is the accuracy with which an operator can set the comparator measuring mark on the calibration scale marks. In the studies of Ref. 3, 4 and 5, the standard deviation of point setting errors on fiducials was on the order of ± 1 micron. Thus, in one out of three measurements, the point setting error would be expected

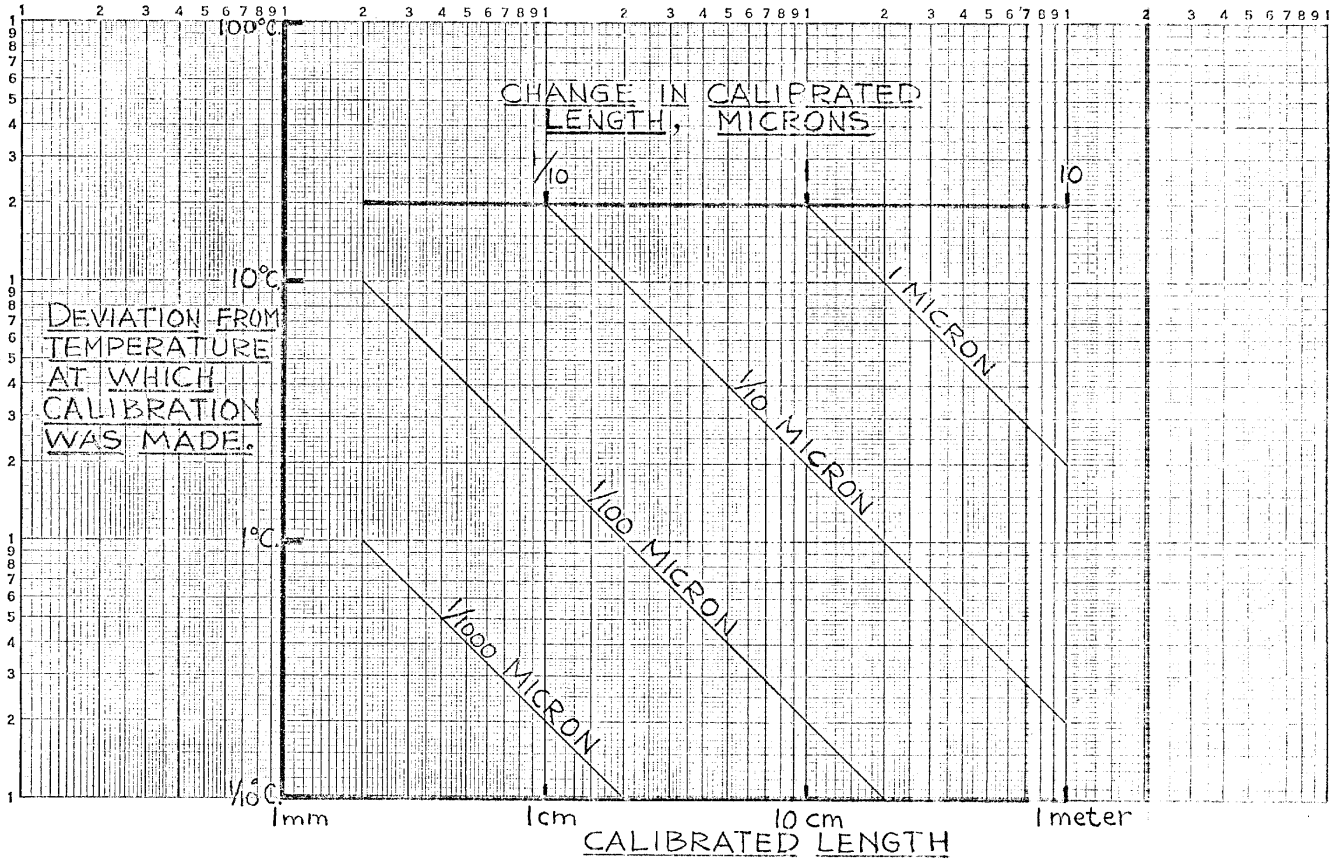

FIG. 2 THERMAL CORRECTION FOR QUARTZ SUBSTRATE

to be greater than 1 micron. Such accuracy would be an unacceptable limitation on the calibration of the High Precision Stereo Comparator. Although there is indication that much better operator point setting precision may be achievable, it has not been proven as yet. It is therefor a controversial question and not suitable for a calibration device.

A technique is required which will permit centering the comparator microscope on the calibration scale graduations to much better accuracy than $\pm$ 1 micron. A proven technique is that used by the Bureau of Standards in calibrating the scales. They achieve point setting precision to a standard deviation of about $\pm$ 0.05 microns, (reference 6).

The Bureau of Standards technique is to scan the image of the scale mark across a slit and with a phototube detect the varying intensity of the light passing through the slit. The output of the phototube is displayed on an oscilloscope and on a meter. Centering on the scale mark can be done manually to good precision by monitoring the oscilloscope and meter display. Very high precision is obtained however by clocking the time the phototube output is above a selected level on the forward scan and on the reverse scan. When the times are equal, the mark is centered. A block diagram of the approach, prepared by Mr. Herbert D. Cook of the Bureau of Standards, Ref. 7, is shown in Fig. 3.

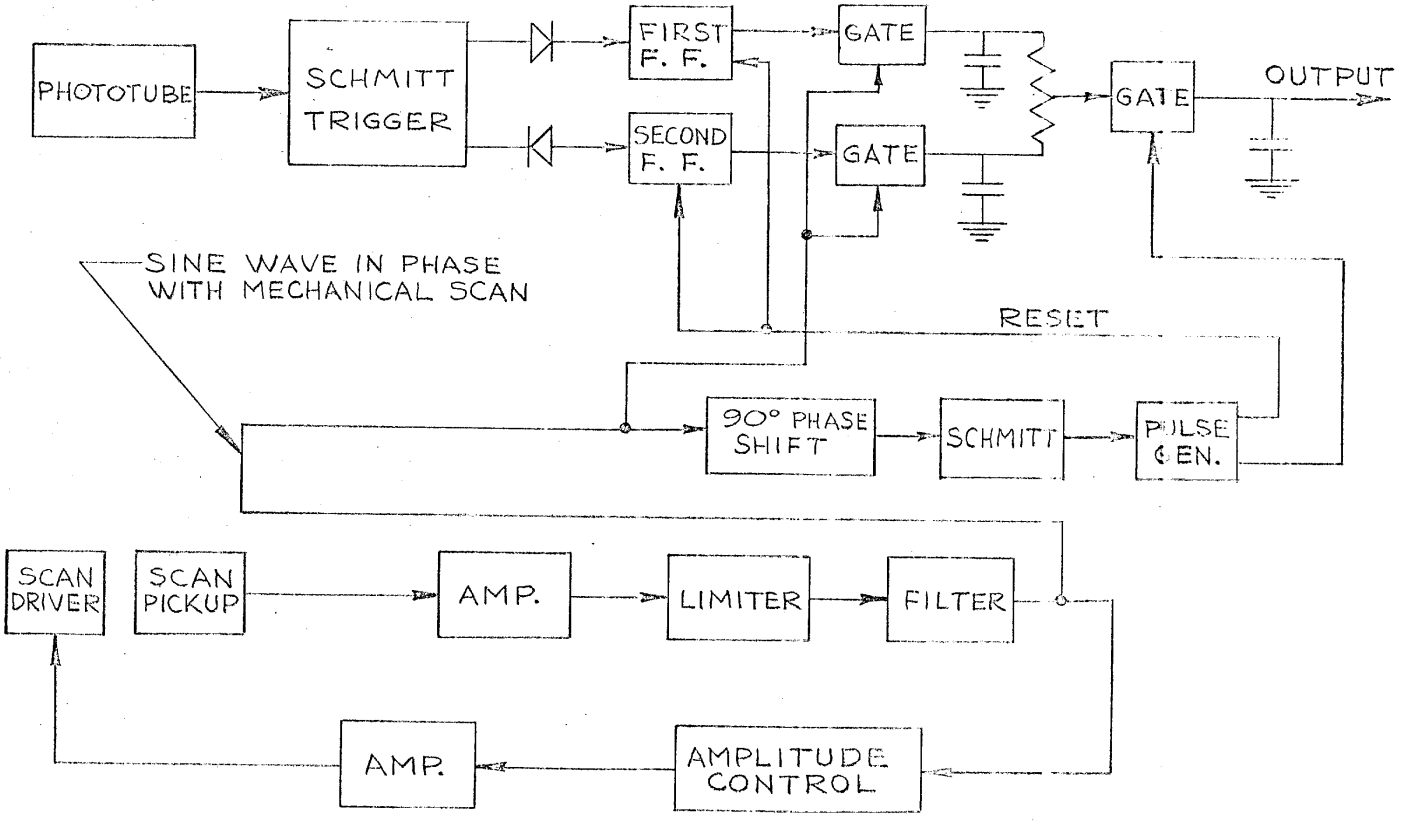

FIG. 3 BLOCK DIAGRAM OF ELECTRONIC POINT SETTING

The Bureau of Standards technique uses a microscope to observe the scale and therefore is readily applicable to precision comparators which use microscopes. For calibrating a precision comparator, it would be desirable to use the comparator microscope to observe the calibrated scale on the comparator platen. Thus all the elements of the normal measuring procedure would be in the calibration procedure.

6. Further Uses of the Calibration Device

Once a calibration device is available and an existing precision comparator has been calibrated, a further investigation of magnitudes of other error sources may be possible.

Errors associated with the properties of film are accesible. Localized film distortions such as occur in non-uniform flattening of the film on the comparator platen and in localized heating of the film by the comparator light source are probably specific to a particular machine. It may be possible to gain insight into the importance of such errors by comparing calibration readings obtained with film substrate and quartz substrate.

Errors associated with operator point setting on fiducials may be accessible by comparing visual point setting calibration readings with electronic point setting calibration readings. Note that positioning of the comparator platen in both cases would be accomplished by the operator using the comparator platen positioning controls.

References

1. Pennington, William and Stewart, Wilton A.; "Laser Metrology". Serrell-Stewart Corporation Report dated February 1, 1966.

2. Mielenz, K. D., Cook, H. D., Billiland, K. E., and Stephens, R. B.; "Accurate Length Measurement of Meter Bar with Helium-Neon Laser". Science, Dec. 25, 1964, Vol. 145, No. 3652, pp 1672-1673.

3. Karara, Dr. H. M; "Mono Versus Stereo Analytical Photogrammetry". Univ. of Illinois Report, Photogrammetry Series No. 9, Feb. 1967.

4. Harabedian, A., Buckner, D. N. and Scott, F.; "The Measurement of Photographic Images by Human Operators", Human Factors Research, Inc., Report March 17, 1967.

5. Ahrend, Martin; "Analysis of Photogrammetric Errors", Carl-Zeiss Werk, Oberkochen, Germany, Report Januray 28, 1966.

6. Private Communication from Mr. John Beers, U.S. Bureau of Standards, Nov. 2, 1967.

7. Private Communication from Mr. Herbert D. Cook, U.S. Bureau of Standards, Sept. 28, 1967.

Appendix A

Definition of "Accuracy" and "Precision".

A measurement, $\hat{l}$, of a linear dimension can be considered to be composed of the true length, l, the bias error, b, and the random error, e, as shown in Fig. 4.

Precision refers to how closely grouped a number of measurements are about the mean value of the measurements. Precision can be characterized by the rms deviation of the measurements about the mean. If the measurements are normally distributed about a mean, then the rms value will be one standard deviation, .

Accuracy refers to how close a measurement is to the true value and includes bias error as well as random error. Accuracy can only be determined if either true length or bias error are known. In establishing procedures to measure the distance between two points, it is advantageous if the bias errors can be made to cancel.

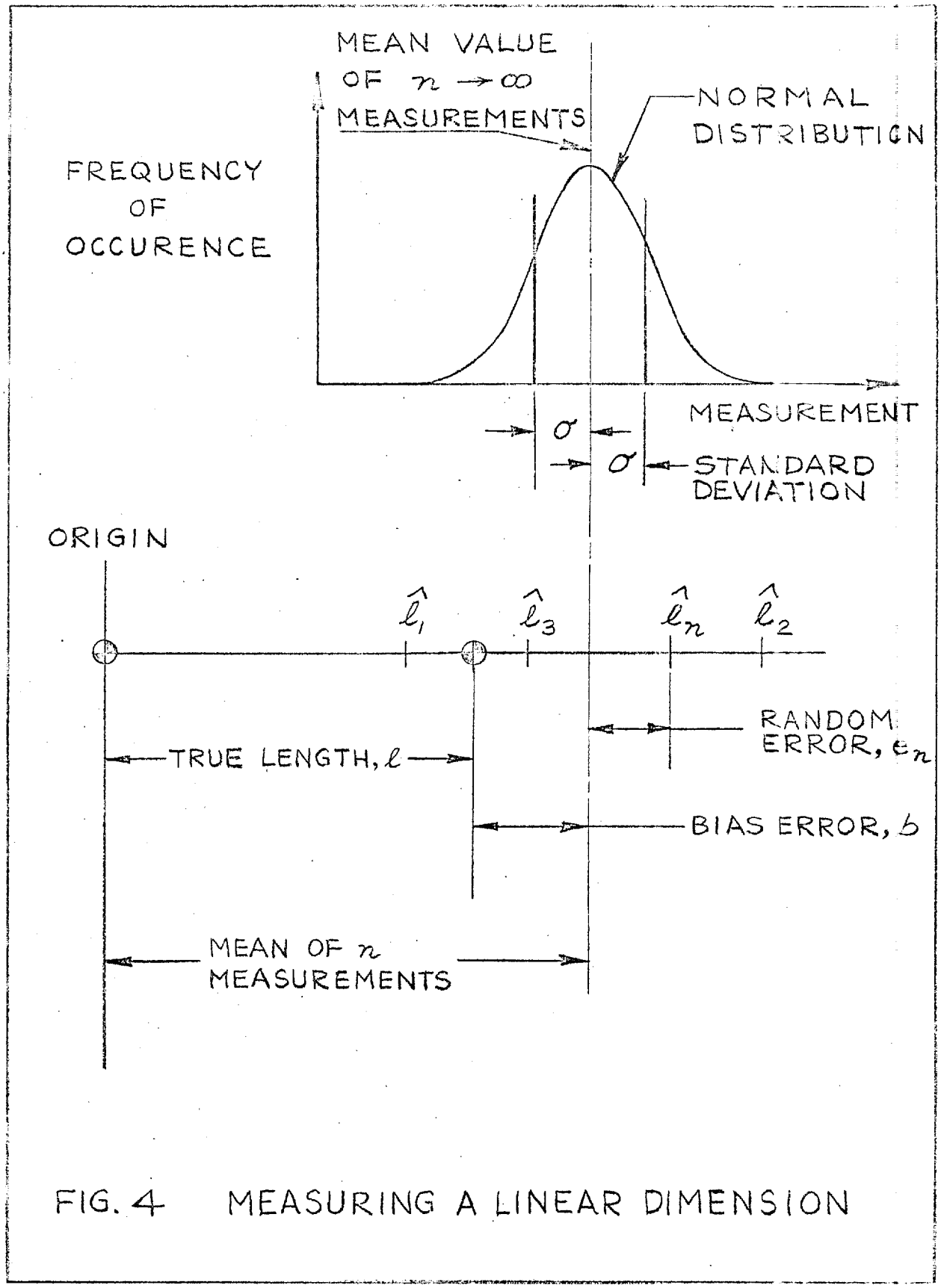

FIG. 4 MEASURING A LINEAR DIMENSION

515088

STAT

TASK 1

the Necessary Accuracy

Research Effort in Support of
High Precision Stereo Comparator

Approved For Release 2005/05/20 : CIA-RDP78B04770A001500040016-6

STAT

November 15, 1967

Mailing Address

STAT

RESEARCH EFFORT IN SUPPORT OF
HIGH PRECISION STEREO COMPARATOR

Task 1 the Necessary Accuracy

Work Statement: An analysis will be made of the accuracies imposed on the machine by the various measuring tasks. Length, angle and other specialized measurements, when computed as a function of point position coordinate measurements, impose their accuracy requirement on the point measurement. Normally, desired accuracies are not achievable and an analysis of errors is required to separate accuracy requirements into constituent factors.

As data becomes available from other studies and other sources, the contribution of operator pointing, film distortion, optical geometry and mission parameters will be included in an analysis of variance. An attempt will be made to determine the relative importance of the error contribution of the measuring machine.

Submitted by,

STAT

STAT [redacted] November 15, 1967

RESEARCH EFFORT IN SUPPORT OF HIGH PRECISION STEREO COMPARATOR

Task 1 the Necessary Accuracy

Contents

STAT [redacted] November 15, 1967

Contents

STAT

November 15, 1967

List Of Figures

STAT [redacted] November 15, 1967

List Of Tables

ACKNOWLEDGEMENTS

STAT [redacted] made the mathematical statistical derivations in the appendices.

STAT [redacted] is a mathematical-statistical consultant in private practice.

STAT [redacted] B.S., M.S., did the basic heat balance work on which Section 3 is based.

SUMMARY

Computation of quantities such as length, angle and area from point position coordinate measurements may be considered as a transformation process. The errors of measurement of image point coordinates are transformed by the computations into errors of the computed quantities. Derivations of the error transformations are given in Appendices A, B and C. Image point coordinate measurements have a statistical distribution of error involving both bias error and random error. (See Appendix D for the definition of bias error and random error.) The transformation of the random error component is a function of the covariance matrix of the x- and y-coordinate random errors.

Computation of length is by far the most important and most extensively used transformation. An examination of variances and covariances shows that the random component of the error in length will range between zero and two times the coordinate error if there is high correlation of the coordinate error and depending on whether they cancel or add. If there is no correlation, then the random component of the error of length will be 1.4 times the random component of the coordinate error. The above involves extreme simplification and the true situation is much more complex. It is discussed more extensively in Section 1 of this report.

Desired accuracy in length measurement is on the order of ± 1 part in 600 (± 1.67 parts per thousand) or $\pm \frac{1}{2}$-foot which ever is larger. The accuracies are equal for a measured length of 300 feet.

The composite of the residual error, after suitable corrections of:

(a) Film thermal coefficient of linear expansion

(b) Film humidity coefficient of linear expansion

(c) Processing shrinkage

(d) Focal length calibration

(e) Fiducial calibration

(f) Obliquity correction,

is only ±0.076 parts per thousand. The composite error is thus not a significant limitation in obtaining the desired accuracy.

Measurement of flying height for the determination of photographic scale appears to be a dominant source of error, especially for measuring long lengths. It becomes nonsignificant only for lengths less than 172 ft.

Note that the accuracy required in the measurement of the distance between fiducials for the purpose of correcting for film dimensional changes is quite relaxed. For the error contribution to be 1/10 the desired accuracy, a fiducial measurement accuracy of approximately ±25 microns is adequate.

Operator point setting accuracy is significant for measuring short lengths, 6½ millimeters or less. It is principally affected by three factors:

(a) Edge spread of the image.

(b) Nature of the image (line, edge or point)

(c) Type of reticle used for pointing.

One curious finding is that magnification, over the range 12x to 80x, has little to do with point setting accuracy. Since such a fact is contrary to intuitive reasoning, the role of magnification in point setting must be a complex one which is not well understood.

The accuracy of existing machines is not known. The least count however is quite adequate for achieving the desired accuracy for measuring lengths greater than 0.6mm. The proposed least count of the High Precision Stereo Comparator is satisfactory and is better than the desired accuracy for all measured lengths.

SECTION 1 MEASUREMENTS

A comparator is used to measure the relative coordinate positions of image points on film. From the coordinate values computations are made of length, angle and area. The procedure is first to establish coordinate origin or zero point. The origin is usually established at a fiducial mark, a reseau cross or some image point on the film. The coordinates of other points are then recorded relative to the zero point. The process of aligning a microscope reticle on the desired image point is one of the major components of the measuring task.

STAT [redacted] have estimated (Ref.5) that such alignment can be made to about one-half a resolution element. Assuming the region of interest in resolution is from 30 lines per millimeter to 200 lines per millimeter, and assuming the approximate relationship that resolution equals the reciprocal of the edge spread, the region of interest in edge spread is from 5 microns to 33 microns. See Fig. 1.

Thus if the reticle can be aligned on the image to one-half a resolution element, then the region of interest in image measurement accuracy is 2.5 to 16.5 microns, shown as region of interest (1) on Fig. 1.

The investigations by Harabedian, Buckner and Scott reported in reference 1, indicate a reticle can be aligned on certain images to about 1/5 the edge spread which is indicated

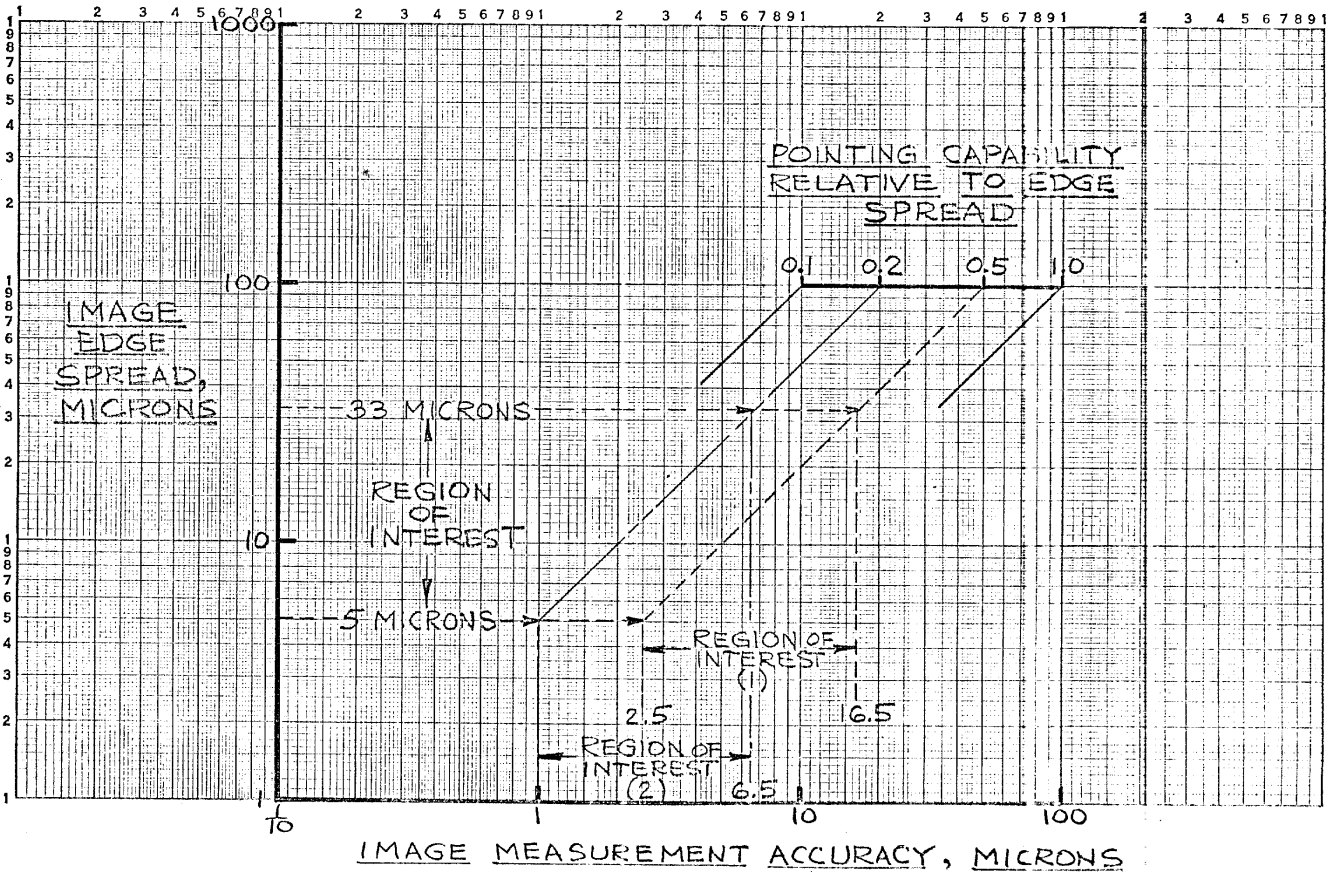

FIG. 1 IMAGE-POINT COORDINATE MEASUREMENT ACCURACY

on Fig. 1 as region of interest (2).

Image-point coordinate measurement accuracy results in certain inaccuracies associated with computed quantities such as length, angle and area. Derivation of the errors in computed quantities is given in Appendices A, B and C.

Errors in computed quantities are composed of bias error and random error. Bias error and random error are defined in Appendix D.

For measurement of length, the bias error, b_ℓ , is:

$$b_\ell = (\cos e_\ell)\ (b_{x2}-b_{x1}) + (\sin e_\ell)\ b_{y2}-b_{y1})$$

where e_ℓ = The angle the measured length makes with the x-axis, and b_{x1}, b_{x2}, b_{y2}, b_{y1} are bias errors of the coordinate measurements. The variance, $\sigma_{\ell\ell}$, of the random error is:

$$\sigma_{\ell\ell} = (\cos^2\theta_\ell)(\sigma_{x1,x1} + \sigma_{x2,x2} - 2\sigma_{x1,x2}) + (\sin^2\theta_\ell)(\sigma_{y1,y1} + \sigma_{y2,y2} - 2\sigma_{y1,y2}) + 2(\sin\theta_\ell)(\cos\theta_\ell)(\sigma_{x1,y1} + \sigma_{x2,y2} - \sigma_{x1y2} - \sigma_{x2,y1})$$

If the variances are equal and defined as σ_c and there is no correlation, this reduces to:

$$\sigma_{\ell\ell} \equiv \sigma_\ell^2 = 2\sigma_c^2$$

The expected value, σ_ℓ , of the random error is then:

$$\sigma_\ell = 1.4\,\sigma_c$$

Similarly, in determining an angle, e, the bias error, will be:

$$b_\theta = \frac{1}{\ell_{1,2}}\left[(\sin\theta_{1,2})(b_{x2}-b_{x1}) - (\cos\theta_{1,2})(b_{y2}-b_{y1})\right] - \frac{1}{\ell_{1,3}}\left[(\sin\theta_{1,3})(b_{x3}-b_{x1}) - (\cos\theta_{1,3})(b_{y3}-b_{y1})\right]$$

If the line segments, $\ell_{1,2}$ and $\ell_{1,3}$ defining the angle, are chosen to be essentially equal in length, then for small angles of θ such that $\sin \theta_{1,2} \cong \sin \theta_{1,3}$ and $\cos \theta_{1,2} \cong \cos \theta_{1,3}$ and the biases are approximately equal, b_c, and do not cancel:

$$b_\theta = \frac{2}{\ell} (\sin \theta_x + \cos \theta_x) b_c$$

at $\theta_x =$ 45° this becomes a maximum:

$$b_\theta \Big|_{\theta = 45^\circ} = \frac{2\sqrt{2}}{\ell} b_c$$

the variance σ_θ^2, of the random error (assuming the coordinate measurement errors are essentially equal and uncorrelated) will be:

$$\sigma_\theta^2 = \frac{2}{\ell^2} (2 - \cos \theta) \sigma_c^2$$

For large angles where $\cos \theta \longrightarrow 0$

$$\sigma_\theta \rightarrow \frac{2}{\ell} \sigma_c$$

For small angles where $\cos \theta \longrightarrow 1$

$$\sigma_\theta \rightarrow \frac{\sqrt{2}}{\ell} \sigma_c$$

In computing the area of a simple figure defined by image points 1 thru n, the <u>bias</u> error will be:

$$b_A = \tfrac{1}{2} \sum_{j=1}^{n} (Y_{j+1} - Y_{j-1}) b_{x_j} - (x_{j+1} - x_{j-1}) b_{y_j}$$

The variance, σ_A^2, of the <u>random</u> error (assuming coordinate measurement errors are essentially equal and uncorrelated) will be:

$$\sigma_A^2 = \frac{1}{4} \left[\ell_{n,2}^2 + \ell_{1,3}^2 + \cdots + \ell_{n-1,1}^2 \right] \sigma_c^2$$

If the line segments are all approximately equal, ℓ_c then:

$$\sigma_A = \frac{1}{2} \ell_c \sqrt{N} \, \sigma_c$$

where N is the number of line segments. N is also the number of points defining the figure.

To summarize, we have seen that errors in determining linear dimensions are on the order of 1.4 times the error in image-point coordinate measurement error. If bias and correlation are unfavorable, the linear length error can be 2 times the image-point coordinate measurement error. The increased error shifts the region of interest to the right on the abscissa of Fig. 1. In Fig. 2, we illustrate the ground object measurement accuracy for a shift of 1.4 to the right of the region of interest (1). The ground object measurement accuracy depends on image quality in terms of edge spread and on image scale. Three scales are illustrated in Fig. 2. For a scale of 1:22,000 with image quality variation from 30 to 64 lines per millimeter, the corresponding ground object measuring accuracy is 1.7 to 0.8 ft. For a scale of 1:37,000 with image quality variation from 64 to 200 lines per millimeter corresponding ground object measuring accuracy is 0.42 to 1.3 ft. For a scale of 1:310,000 with image quality variation of 64 to 125 lines per millimeter, the corresponding ground object measuring accuracy is 5.8 to 11 ft.

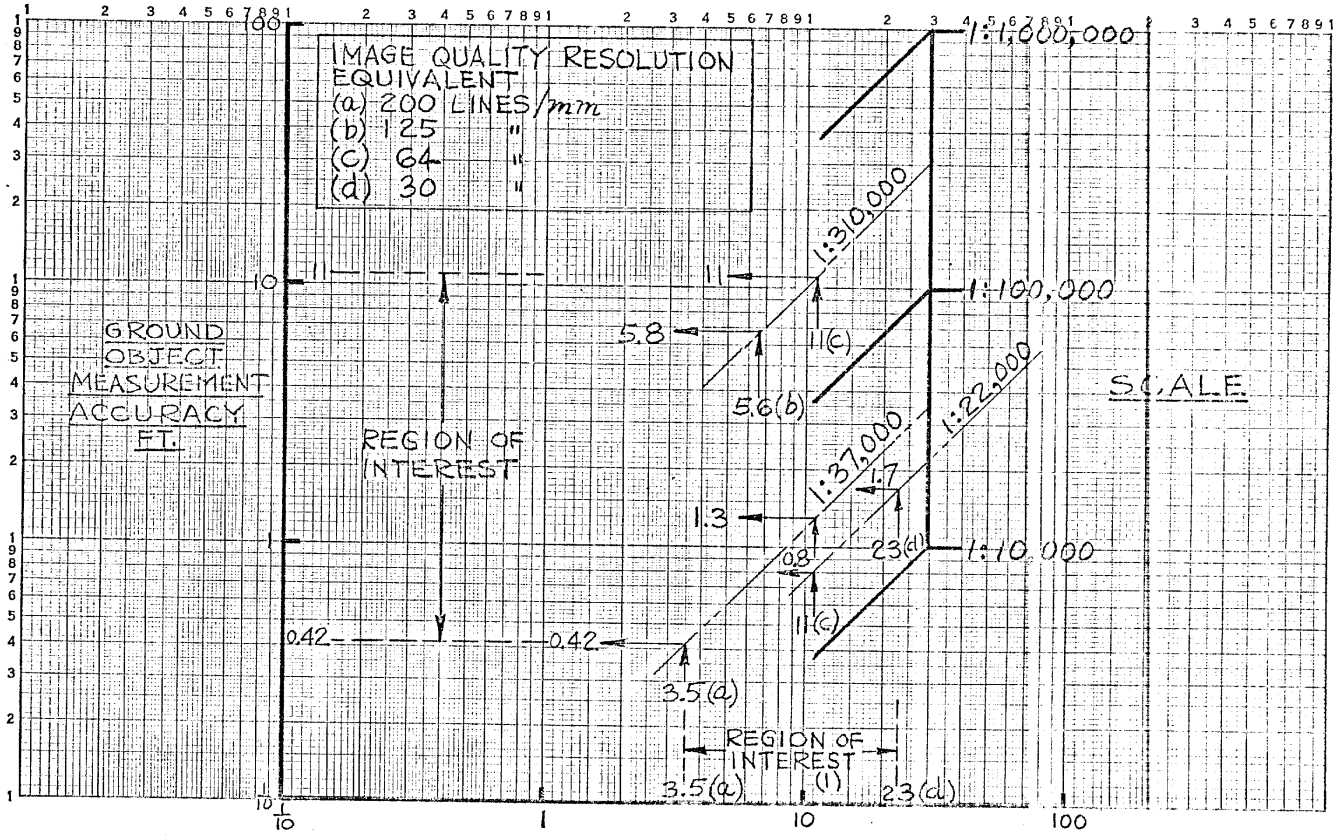

LINEAR DIMENSION MEASUREMENT ACCURACY, MICRONS

FIG. 2 GROUND OBJECT MEASUREMENT ACCURACY

Fig. 3 illustrates the implications of the region of interest in the measurement of ground objects. Under the best conditions, an 8 ft. vehicle width could be measured to 1 part per 20; a 42 ft. truck length could be measured to 1 part per 100; a 250 ft. ship could be measured to 1 part per 600. Following the 1 part per 600 line means that a 6,500 ft. runway could be measured to 11 ft. or better.

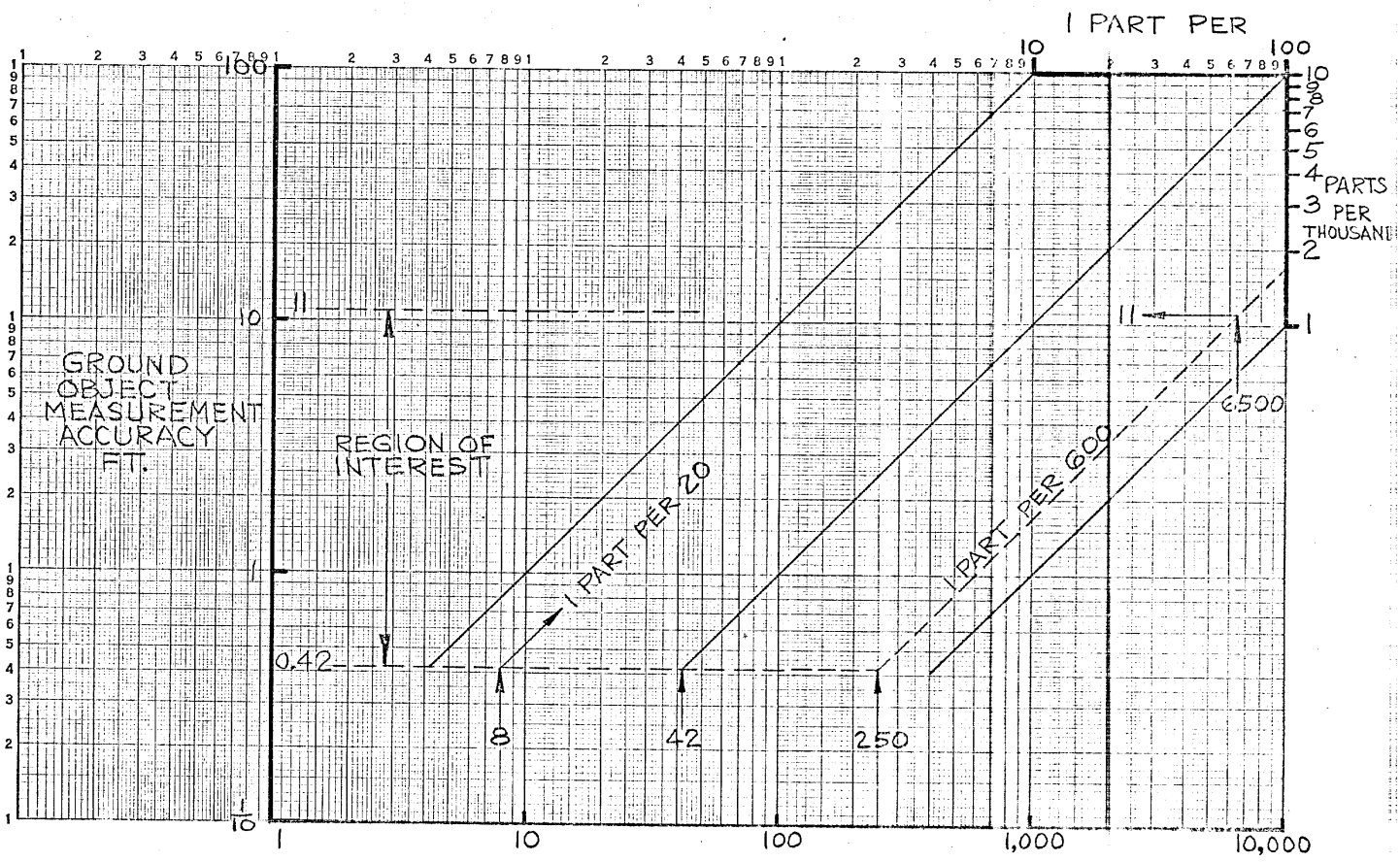

FIG. 3 GROUND OBJECT DIMENSIONS

SECTION 2 OPERATOR POINT SETTING ERRORS

The principal factors affecting the accuracy with which an operator can set a measuring mark or reticle on an image point are the edge spread of the image point, the nature of the image point (i.e. line, straight or curved edge, acute or obtuse angle) and the nature of the reticle.

It appears that contrast affects point setting accuracy only if it is very low, approaching threshhold values.

The role of magnification is not clear and must be more complex than simple intuitive deduction would conclude.

Under idealized conditions, it appears that an operator can set points far more accurately than any existing or contemplated comparator.

Each of these aspects will be discussed in detail in this section.

2.1 Edge Spread

In the study by Harabedian, Buckner and Scott, Ref. 1, edge spreads of 5 to 24 microns* were used

*Using the approximate formula for converting edge spread to resolution, 1/edge spread in mm= resolution in lines/mm, the equivalent resolutions are 200 lines/mm to 42 lines/mm.

to determine standard deviations of pointing errors. In addition a master plate was used on which the edge spread was not known but was very much less than 5 microns. For edges of good contrast (above 0.15 modulation) which were curved or straight, they obtained the results shown in Table I.

In this discussion we are not considering the point setting error data in the Ref. 1 report for pointed edges, (vertices of angles), as that data has distinct and separate significance.

It appears from Table I that the random error (the standard deviation) generally increases as the edge spread increases. I would suspect though, that the trend is contaminated at the smaller edge spreads by the machine accuracy. The bias error does not evidence a consistent trend. Again I suspect the bias error up to 16 3/4 micron edge spread is merely machine error and that only at the 24 micron edge spread does operator point setting bias show up. From Table II we see that point setting can be accomplished to about 1/7 to 1/4 the edge spread for the larger edge spreads. We cannot be certain however that a more accurate machine would permit maintaining the same ratio for smaller edge spreads.

2.2 Nature of the Image and Ideal Conditions

Studies (Ref. 1,2 and 3) indicate that operator point setting accuracy depends upon whether the image is a line, an edge, or a point (defined as the vertex of an angle).

TABLE I

Point Setting Accuracy
Versus Edge Spread

Edge Spread In Microns	Standard Deviation of Point Setting (X-Coordinate only), Microns	Bias, Microns
Master Plate Fiducials	1.0	
Master Plate Edges	1.4 to 2.1	defined as zero
5	1.2 to 2.6	-0.6 to-0.8
7 1/2	1.6 to 2.9	-1.5 to -1.6
11 1/4	1.6 to 3.6	+0.3 to -0.9
16 3/4	2.2 to 3.7	+0.7 to -0.3
24	3.7 to 6.4	-2.3

Conditions

6 operators made three point settings each on 21 separate curved or straight edges for three contrasts for each edge spread. (Note, the extreme low contrast edges are not included in the above data). Measurements were made with the Mann 621 comparator. Magnifications of 40x to 80x were used and were selected by the operator.

However, the length of the line or edge, the curvature of the edge and the contrast of the image have a very wide range over which they do not affect point setting accuracy. Apparently only at threshhold values do they have an appreciable effect.

In D. C. O'Connor's work Ref. 4, it is shown that the design of the measuring mark (reticle) affects operator point setting accuracy in a major manner. He was able to demonstrate with a simple, specially designed apparatus that an operator's point setting accuracy was far better than any existing or contemplated comparator accuracy.

The data is summarized in Table III and various reticles illustrated in Fig. 4. Note that for a line image, point setting accuracy is 0.8 to 1.0 microns. I would strongly suspect that the accuracy is limited by machine capability and not by operator pointing capability. The reticles used were of the type illustrated in Fig. 4 (a) and (b). The most effective arrangement is that shown in Fig. 4 (c) in which the operator can balance the clear space on the left between the fiducial mark and the reticle bar against the clear space on the right. It may be that an operator uses an energy balance mechanism to achieve accuracies far better than that of eye resolution. Integration of the energy for a few seconds may make very small differences detectable. O'Connor used artificial reticles of the type shown in Fig. 4 (d). Note that x-coordinate position measurement was achieved by left-right balancing of the clear space between the measuring mark and the hole and y-coordinate position measurement was

TABLE II

Ratio of Point Setting
Accuracy to Edge Spread

Edge Spread In Microns	Ratio of Point Setting Standard Deviation to Edge Spread
5	0.24 to 0.52
7 1/2	0.21 to 0.39
11 1/4	0.14 to 0.32
16 3/4	0.13 to 0.22
24	0.15 to 0.27

TABLE III

Nature of the Image
and Point Setting Accuracy

	Artificial Points	Lines Images	Edge Images	Vertices of Angles 22^{o} to 135^{o}
Martin Ahrend (Ref 2)				
Reseau Crosses		1.0		
White Boundary Points				
Mono			1.6	
Stereo, x-Direction			2.9	
Stereo, y-Direction			3.3	
Harabedian, Buckner & Scott (Ref 1)				
Fiducials		1.0		
Straight & curved edges				
Master Plate			1.4 to 2.1	
Edge Gradient 24 microns			3.7 to 6.4	
Pointed Edges				
Master Plate				1.4 to 4.1
Edge Gradient 24 microns				4.2 to 20.5
H. M. Karara (Ref 3)				
Fiducials		0.8		
Wild Pug Point				
Transfer Mark				
x-Direction	2.2			
y-Direction	2.4			
D. C. O'Connor (Ref 4)				
Artificial Measuring Mark and Concentric Point Transfer Mark	½ arc sec.*			

* Equivalent to 1/20 micron at 12x magnification.

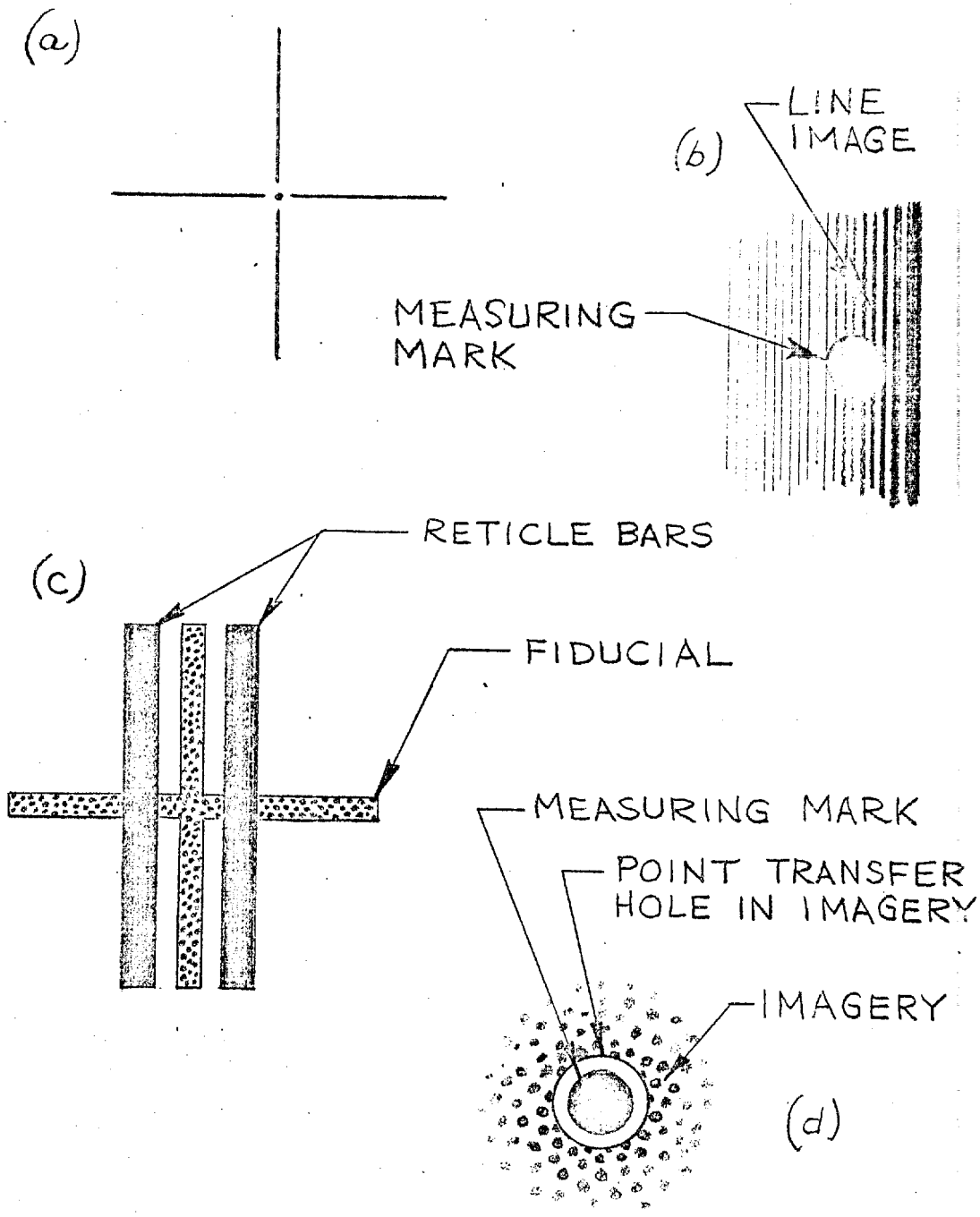

FIG. 4 RETICLES

achieved by up-down balancing of the clear space between the measuring mark and the hole. Although limiting eye resolution is usually taken to be about 1 arc minute, O'Connor found that centering capability was 120 times better, i.e. ½ arc second.

2.3 Magnification

Intuitive reasoning would indicate that operator point setting accuracy should be directly proportional to viewing magnification. The test data of references 1,2,3 and 4 do not bear this out. In the reference 1 investigation, operators were permitted to select the most convenient viewing magnification in the range of 50x to 80x. There was no discernable trend in point setting error related to magnification. The least error was that for fiducials which amounted to about 1 micron. The error for sharp edges was about 2½ microns. In the reference 2 work, the viewing magnification varied from 1x to 200x. The point setting mean square coordinate error for reseau crosses was 1 micron and for image boundary points it ranged from 1.6 to 3.3 microns. In one set of data in which a viewing magnification of 16x was used, the point setting error on image boundaries was 1.6 microns. In the reference 3 work magnification of 20x was used throughout. An average standard deviation of 0.8 microns was obtained for fiducials. For image points the average standard deviation ranged from 1.9 to 2.5 microns.

In none of this work was there any attempt to correlate point setting with the dimension of the edge spread as referenced to the retina of the eye. There may be some optimum size, however the optimum could be very broad. In reviewing the Ref. 1 data, no optimum size of the edge on the retina was apparent.

O'Connor showed, Ref. 4, that when a right, left or up down balance arrangement prevailed, operator point setting accuracy was extraordinarily good. It maybe that the physiological mechanism involved is an energy balance rather than a dimensional balance and hence is only weakly dependent on viewing magnification.

It appears that magnification and reticle design is one of the most fruitful areas of investigation for potential improvement in measuring accuracy.

SECTION 3 FILM DISTORTION

3.1 Correctible Distortions

Certain film distortions are amenable to application of correction factors. If dimensional changes of the film are uniform over a full frame and if the taking camera has calibrated fiducials recorded on each frame, then measurement of the fiducials on the film provides a correction factor for image measurements. Several sources of film size change can be corrected in this manner.

(a) Thermal environment
(b) Humidity environment
(c) Processing
(d) Aging
(e) Tension

The approximate magnitude of the dimensional changes is presented in Table IV. The significance of the changes is illustrated in Fig. 5. Note that if the environmental changes and tensions are small, no correction is even necessary. Processing and aging shrinkage, however, is significant and correction factors should be utilized.

Note that the correctible distortions, if uncorrected, may be considered to be principally bias errors in measured lengths.

When corrections are applied by measuring camera fiducial marks on the film, the residual error will be composed of both random and bias errors.

TABLE IV

APPROXIMATE FILM DIMENSIONAL COEFFICIENTS

	Parts Per Thousand		
	Estar Thin Base Type 4401	Triacetate Thin Base Type 8402	
		Length	Width
Thermal Coefficient of linear expansion, per degree F., reversible.....	0.15	0.025	0.035
Humidity Coefficient of linear expansion, per 1% R. H., reversible.....	0.035	0.080	0.100
Processing coefficient of linear expansion (shrinkage), irreversible.....	-0.200	-1.000	-1.000
Processing plus long term aging, coefficient of linear expansion (shrinkage), irreversible.....	-0.500	-2.000	-2.200
Tension coefficient of linear expansion, per p.s.i., reversible.....	0.00154	0.00182	

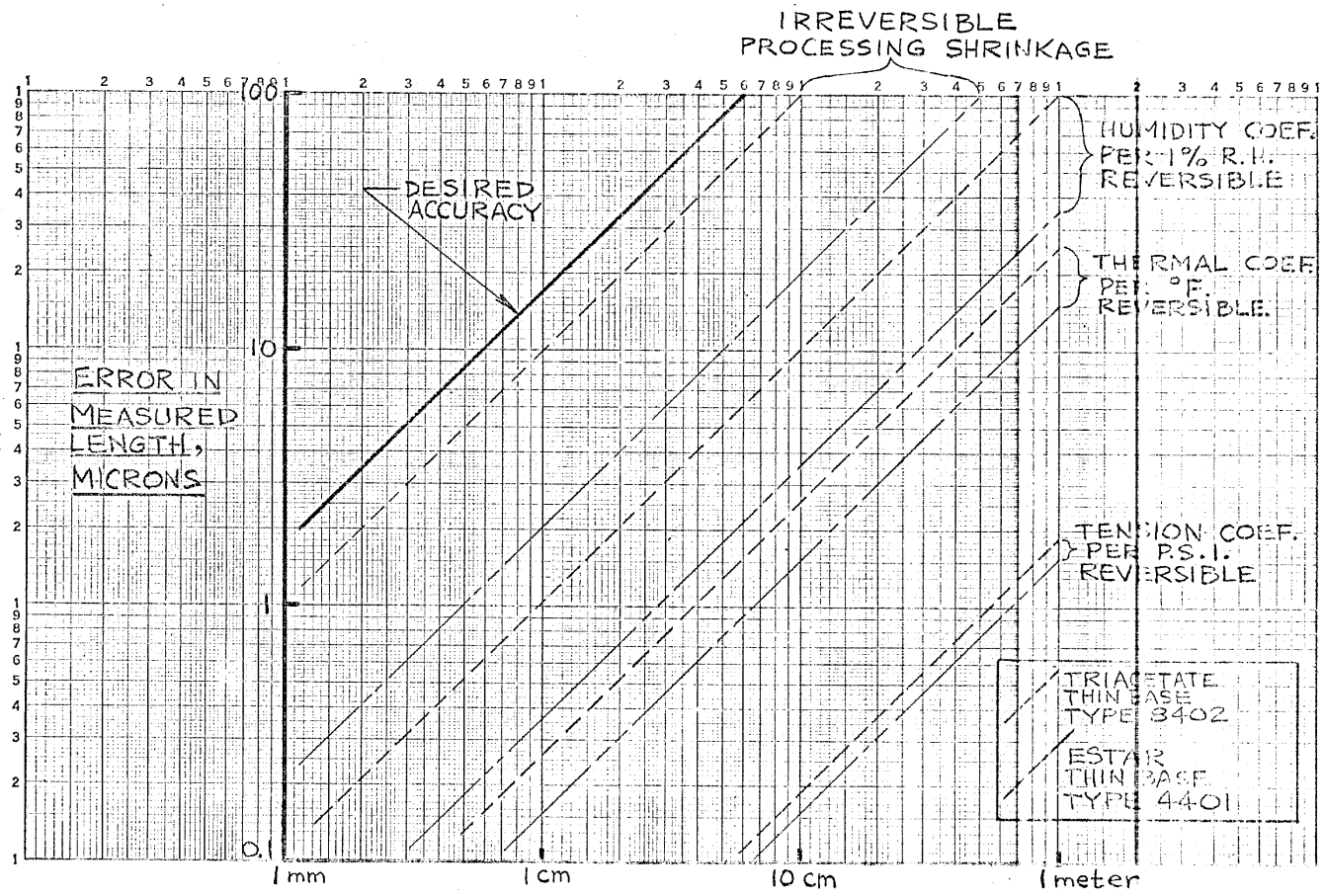

FIG. 5 CORRECTIBLE FILM DISTORTION

3.2 Uncorrectible Distortions

Certain film distortions resulting from the effect of the comparator on the film and which only affect localized portions of a frame may be considered to be presently uncorrectible distortions. There are two principal sources:

(a) Non-uniform flattening of the film on the platen

(b) Localized heating of the film by the comparator lamp.

The magnitude of the distortion from the first source is completely unknown. It may vary from machine to machine and from time to time on a particular machine. In flattening the film on the platen, a bubble of trapped air may form between the film and the platen. As air slowly escapes from the bubble, plastic flow of the film enables it to flatten itself against the platen. A very rough approximation of the magnitude can be obtained by assuming the film distortion is approximately equal to the ratio of the height of the bubble to the radius of the bubble. Thus if the bubble is 0.1 mm high and 25 mm radius, the film distortion resulting from flattening the bubble would be about 1 part in 250. Distortions of this magnitude are significant. Extreme care should be taken in design of the comparator vacuum pull down system and in the usage of the comparator to insure that bubbles do not form.

Some insight into the magnitude of the distortion from the second source may be gained from Ref. 8. Comparators generally use a lamp and some form

of condenser optics to illuminate a small area of film under the microscope. The first case to consider is that in which the illuminated area of the film is constant and does not change as the power of the viewing microscope is changed. For a constant radiation flux density, 1 watt per square inch, absorbed by the film and assuming a simplified one-dimensional steady state model with conventional forced air cooling, the dimensional coefficient will be (see Ref. 8):

0.156 parts per thousand for thin base estar type 4401

0.262 parts per thousand for length change in thin base acetate, type 8402

0.366 parts per thousand for width change in thin base acetate, type 8402.

The second case to consider is that in which the illuminated area of the film is changed as the power of the viewing microscope is changed so that a constant brightness is maintained in the microscope image. For a constant total radiation, the flux density varies as the illuminated area changes and the coefficient of linear expansion also changes. Fig. 6 illustrates the coefficient of linear expansion versus illuminated area per watt of absorbed radiation. The actual physical case is far more complex than is presented here. The film distortion is a two-dimensional transient problem which requires a high speed digital computer to obtain numerical solutions. For a fuller treatment see reference 8.

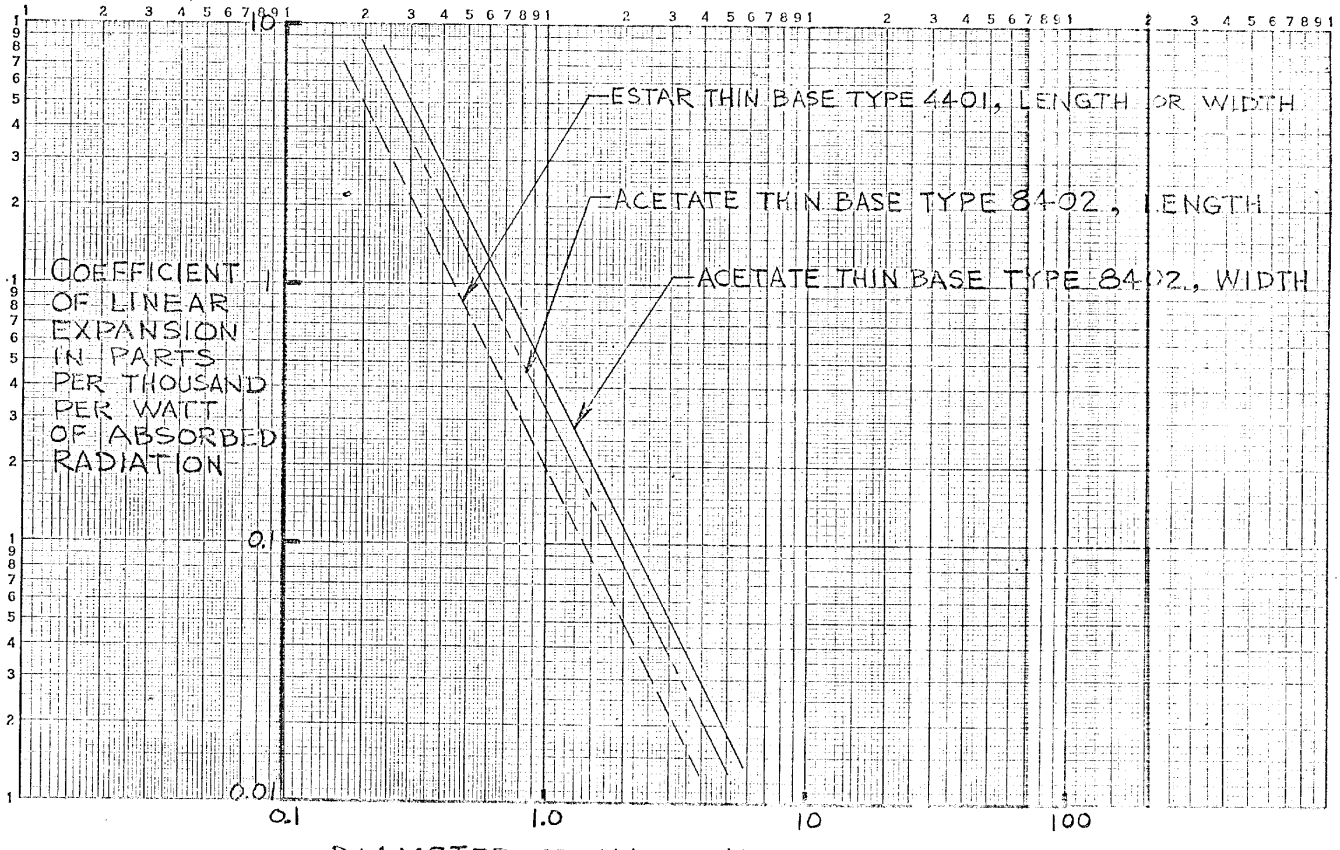

FIG. 6 COEFFICIENT OF LINEAR EXPANSION PER WATT OF ABSORBED RADIATION

SECTION 4 OTHER ERROR SOURCES

4.1 Camera

In the taking of aerial photographs, there are several sources directly associated with the camera which contribute to errors in mensuration. For example:

(a) Fiducial mark calibration
(b) Lens focal length calibration
(c) Optical distortion
(d) Platen unevenness

In some cases both fiducials and focal lengths are reported to a least count of 1 micron (40 microinches). Precision shop practice should readily permit measurement of fiducials on the camera to 0.0001 inches. For a 9-inch format, this is equivalent to about 0.011 parts per thousand.

Since focal length calibration is a "simple coefficient" (see Section 5), calibration to better than 0.01 parts per thousand is meaningless in relation to a desired accuracy of 1.67 parts per thousand. Thus the necessary focal length calibration accuracy need be no better than:

Lens Focal Length	Allowable Calibration Error
6 - inch	± 1.52 microns
18 - inch	± 4.56 microns
160 - inch	± 40.6 microns

Optical distortion is a hybrid type of error. For a framing camera it is generally

considered to be a coordinate correction and is a function of polar coordinates with the origin at the optical axis. Corrections are usually assigned by zones of the format. Although the corrections may not be large they can be significant for cartographic measurements covering nearly a full format. For localized measurements of a small image, it is not so much the correction itself as the first derivative of the distortion function which is important. Although there is little information on the first derivative of the optical distortion function, we know that the function is a continuous slowly varying function of small magnitude, therefore we can conclude that the first derivative will be very small and for our purposes probably not significant.

For a panoramic camera, optical distortion is principally a scale distortion and is a function of camera angle. For simplicity it may be considered an obliquity type error which will be discussed later.

Platen unevenness is included for the sake of completeness. Little information is available regarding its magnitude or its effect on measuring accuracy. Ahrend, in reference 2, gives values of 0.4 to 1.7 microns mean square coordinate error for pressure plate unevenness from measurements of 140 pressure plates. Ahrend's data however is not necessarily applicable to reconnaissance type cameras. We would not expect measurement error due to platen unevenness to be significant.

4.2 Camera/Vehicle System

The principal measurement error sources related to the camera/vehicle system are:

(a) Flying height determination
(b) Atmospheric disturbances
(c) Geometry of exposure

The flying height determination directly affects scale and is a "simple coefficient", (see Section 5). Flying height is reported, per reference 9, to an accuracy of 2.9 parts per thousand. It appears that it is the dominant error for measurements greater than about 4mm referred to the film plane.

The contribution of atmospheric disturbances to mensuration error has not been isolated. The wide variety of conditions and the multiplicity of combinations makes useful analysis extremely difficult. Indications are that under good conditions the contribution of atmospheric disturbances is not significant.

The geometry of exposure depends on such characteristics of the camera/vehicle system as:

(a) Pan or fixed format
(b) Focal plane or intra-lens shutter
(c) Residual errors in stabilization
(d) Residual errors in image motion compensation
(e) Side oblique angle
(f) Forward or aft tilt angle
(g) Aircraft roll, pitch and yaw angles
(h) Timing mark time variation

While their contribution to mensuration error is amenable to analysis, they tend to be specific to a particular camera/vehicle system thus a detail analysis is not suitable for this report. In general we can say that the geometry factors are applied as corrections to measured (computed) lengths and thus are simple coefficients. To obtain some estimate of the expected magnitude, we can make a sweeping simplification that the principal result of geometric factors is an obliquity correction. The error in measured length is therefore a (1-cos) function of the error in obliquity angle. Assuming the geometry of exposure can be reconstructed to about $\pm\frac{1}{2}$-degree, then the error contribution will be ± 0.04 parts per thousand.

4.3 Printing

Mensuration errors associated with printing are a function of contact (or lack thereof) between the negative and positive and the geometry of the light source. Ahrend, Ref. 2, reports a mean square coordinate error of ± 1.7 microns for contact printed diapositive plates. In measurement of 23 plates, the variations were from 0.8 to 3 microns. This data is not applicable to continuous film printers. For printers in which the positive and negative are passed over a drum, a coefficient type error is produced which is a function of the ratio of film thickness and the radius of curvature. For motion picture work (Ref. 10) in which a 12-inch circumference drum

is used for 5.5 mil film the coefficient is about 0.3%. For thin base film and larger drums, we can expect the coefficient to be on the order of 0.5 parts per thousand.

SECTION 5 COMPOSITE ERROR

5.1 Simple Coefficients

There is a class of errors which may be considered as simple coefficients. This class will be defined as those factors which affect the whole format uniformly and which are constant during a sequence of measurements. In other words they introduce bias error coefficients. Examples of simple coefficients are processing shrinkage, and scale factors in framing cameras. We call the factors coefficients because they are dimensionless and are expressed in percent, parts per thousand or parts per million.

Temperature and humidity coefficients may be considered simple coefficients to the extent that the ambient conditions do not change during measurement and the film is in equilibrium with the environment. Table V lists all of the simple coefficients for which numerical examples are available or can be estimated. While it is true that the coefficients are not a function of image coordinates or of a sequence of measurements within a set, they may very well vary from frame to frame or from day to day. Since the constituent factors of the list are independent inputs, the expected value of the variance of the composite error will be the sum of the variances of the input errors. The expected value of the composite error will thus be the square root of the sum of the squares of the input errors. Note that the error in altitude determination is dominant.

TABLE V

SIMPLE COEFFICIENT, NUMERICAL EXAMPLES

Residual Error in Constant Factors
Applied to Linear Measurement

	Parts per Thousand
Thermal coefficient of linear expansion, E.K. estar thin base film type 4401, corrected to ±1°F.	0.015
Humidity coefficient of linear expansion E.K. estar thin base film type 4401, corrected to ± 1% R.H.	0.035
Processing plus long term aging coefficient of linear expansion, E.K. estar thin base film type 4401, corrected to 10% of processing shrinkage.	-0.05
Continuous roll pringtin corrected to ± 10% of the circumference differential.	0.05
Focal length calibration error.	0.01
Altitude determination.	2.9
Fiducial calibration error.	0.01
Air temperature error in wavelength of laser interferometer measuring element assuming no correction over a ± 10°F temperature variation.	-0.005
Barometric pressure error in wavelength of a laser interferometer measuring element, assuming no correction over ± 25mm Hg (±1-inch Hg) barometric pressure variation.	0.009

(The estimated error coefficient is based on Ref. 9) The composite error of all the other factors is ±0.076 parts per thousand. The composite error, including altitude is ±2.90.

The relationship to the desired accuracy is shown graphically in Fig. 7.

5.2 Summary of Errors

Operator point setting discussed in Section 2 is a type of error which is not a coefficient. The error contribution is a point position error and over a reasonable range is not a function of the measured length. For a conservative estimate of magnitude, let us look at the point setting error for a line with an edge spread of 5 microns (assumed equivalent to about 200 lines per millimeter) and for a line with an edge spread of 33 microns (assumed equivalent to about 30 lines per millimeter). From the experimental evidence for 5 micron edges, we are not justified in assuming a positioning capability better than one-half the edge spread. Thus the expected rms error on a measured length will be about 3.5 microns. From the experimental evidence for large edge spreads however, the positioning capability will be at most one-fourth the edge spread. Thus the expected rms error in a measured length with 33 micron edge spread will be 10.5 microns. This error is a limitation on desired accuracy only for measured lengths of 6½-millimeters or less.

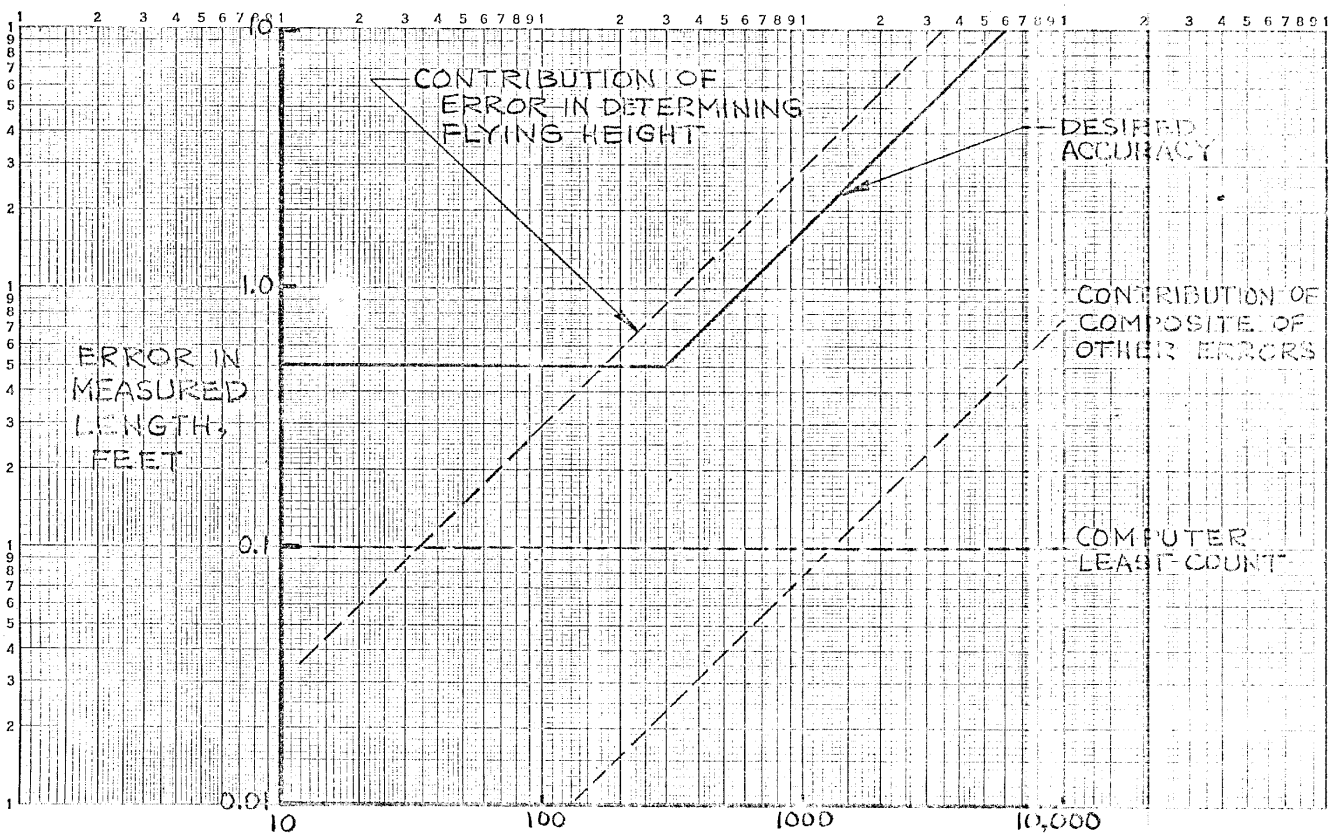

FIG. 7 SIMPLE COEFFICIENT ERRORS

In Fig. 8, the various errors are presented to show their relationship to desired accuracy. A measured length of 6½-millimeters appears at first thought to be unusually small. Fig. 9, shows however, that it is equivalent to ground dimensions on the order of 468 ft. to 6600 ft., depending on scale. Since dimensions of most objects of interest, vehicles, buildings, ships, are less, it is clear that operator point setting limits the accuracy of their measurement.

The absolute accuracy of existing machines is not well known. The least count of the Mann Comparators is 1-micron and as can be seen from Fig. 8, is suitable for nearly all measuring tasks. The proposed least count of the High Precision Stereo Comparator, 0.3164-microns is fully adequate.

In Table VI are collected numerical examples of the errors introduced by these and other factors.

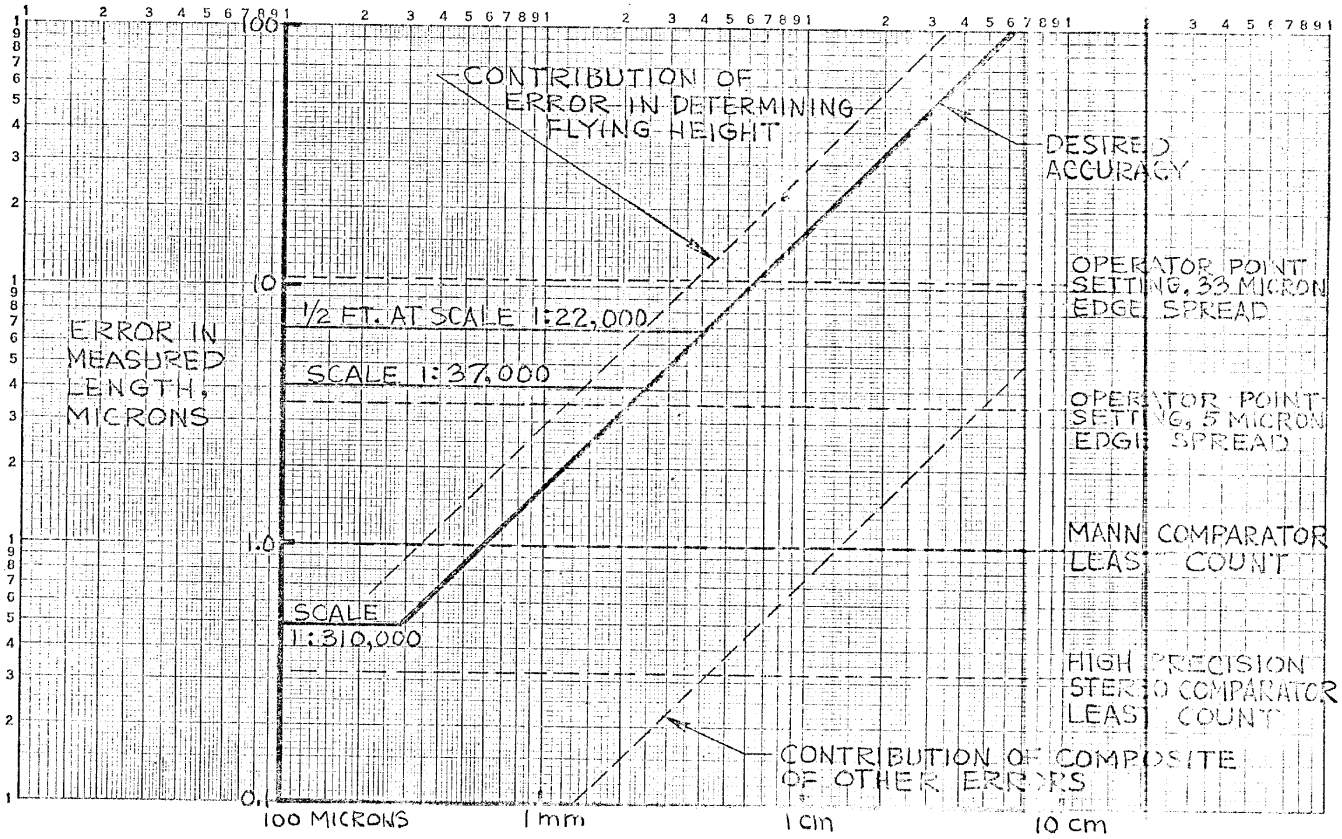

FIG. 8 SUMMARY OF ERRORS IN IMAGE MEASUREMENT

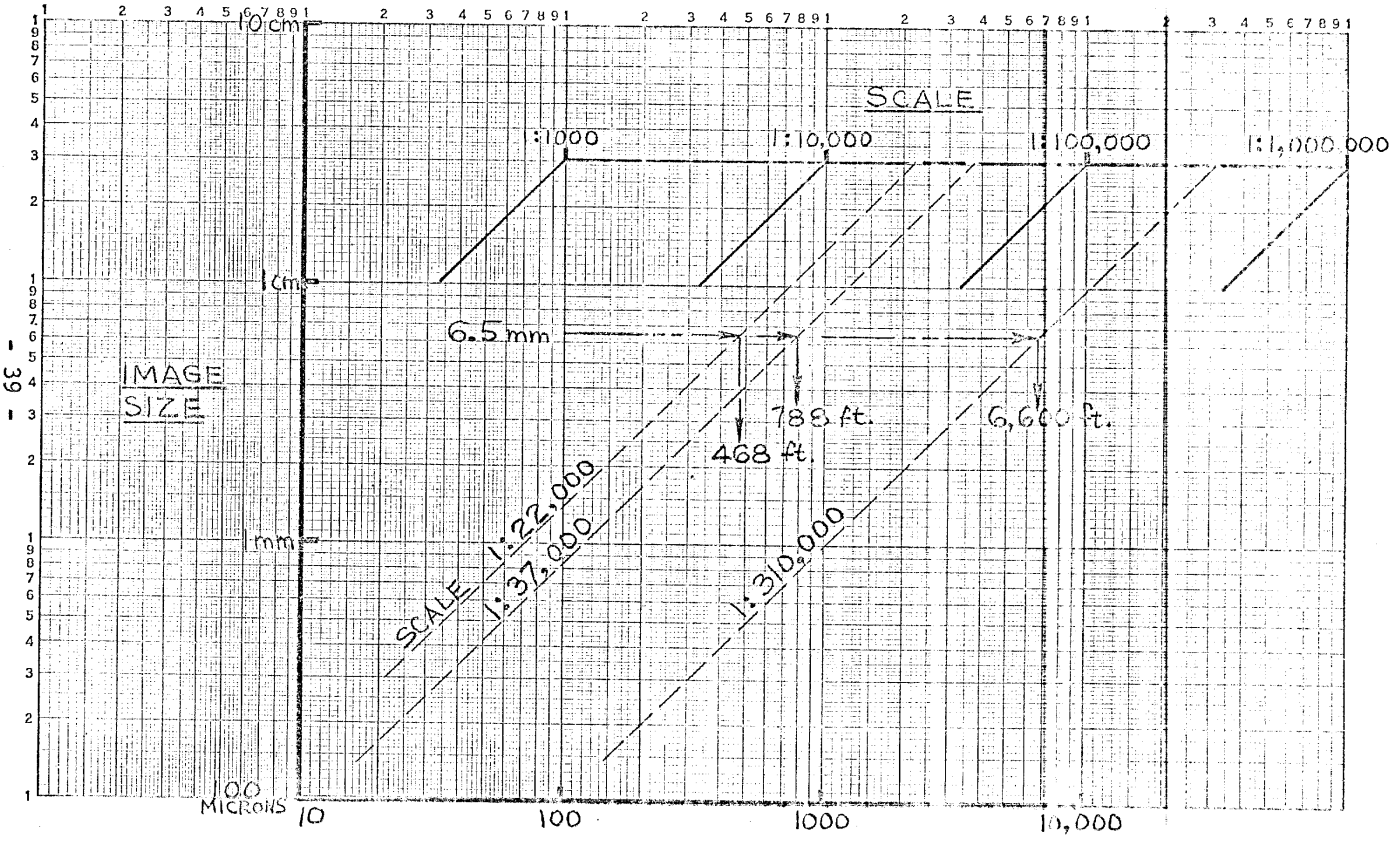

FIG. 9 IMAGE SIZE vs. GROUND OBJECT SIZE

TABLE VI

OTHER FACTOR ERRORS, NUMERICAL EXAMPLES

Operator Point Setting Capability	3.5 to 10.5 microns
Comparator least count	0.3 to 1.0 microns
Computer least count, 0.1 ground ft. at 1:310,000 to 1:22,000 scale	0.098 to 1.39 microns
Vacuum pull down errors (for a bubble 25mm radius and 0.1mm high)	unknown (4 parts per thousand)
Localized thermal distortion, not well known, possibly on the order of	0.1 to 10 parts per thousand per watt

SECTION 6 CONCLUSIONS

(a) Error in measuring length is 1.4 times the error in measuring coordinates, (for simplifying assumptions).

(b) The desired accuracy is readily attained by machines and operators for lengths greater than 6½ millimeters (¼-inch).

(c) The desired accuracy is limited by operator point setting for lengths less than 6½ millimeters (¼-inch).

(d) The dominant error is the determination of flying height. The contribution of the composite of other errors is very small and does not limit desired accuracy. The composite of other errors is the residual error after applying what are believed to be reasonable corrections.

(e) Only for measuring very short lengths (less than 1mm) and at small scales do existing machines fail to achieve desired accuracy.

(f) Assuming the High Precision Stereo Comparator attains a measuring accuracy equivalent to the proposed least count, it will be adequate for all present and forseeable measuring tasks.

SECTION 7 RECOMMENDATIONS

The most fruitful course of future actions is three-fold:

(a) Find ways to improve operator point setting accuracy for measurements of a few millimeters or less. There are several promising leads for attaining significant improvement.

(b) Make a thorough study of error sources to be assured that there are no other dominant inputs. Without deeper penetration, we cannot assume that flying height measurement is the dominant source of error.

(c) Exploit the findings by establishing new methodology for the primary measuring tasks. There are several promising leads for making significant reductions in equipment costs.

References

1. Harabedian, A., Buckner, D. N., and Scott, F.; "The Measurement of Photographic Images by Human Operators". Human Factors Research, Inc., Santa Barbara, Calif., Report. March 17, 1967.

2. Ahrend, Martin; "Analysis of Photogrammetric Errors". Zeiss, Oberkochen; Jan. 28, 1966

3. Karara, Dr. H. M.; "Mono versus Stereo Analytical Photogrammetry". University of Illinois.

4. O'Connor, D. C.; "Visual Factors Affecting the Precision of Coordinate Measurements in Aero-triangulation". Univ. of Illinois, Doctoral thesis, 1967.

5. Private Communication from [redacted] STAT September 29, 1967.

6. Physical Properties of Kodak Estar Base Films, Eastman Kodak Company, Rochester, N.Y.

7. Manual of Physical Properties of Kodak Aerial and Special Sensitized Materials, Eastman Kodak Company, Rochester, N. Y.

8. Yu, Ying-nien; "The Contribution of Film Distortion", Serrell-Stewart Corporation Report dated Sept. 18, 1967.

9. Private Communication from Mr. Mort Brown, Sept. 27, 1967.

10. "Proposed American Standard Dimensions for 35mm Motion Picture Film", PH 22.102 J. of SMPTE V72, p.111. Feb. 1963.

List Of Symbols

True length of a line	ℓ
Measured length of a line	$\hat{\ell}$
True coordinates of point 1	x_1, y_1
True coordinates of point 2	x_2, y_2
Measured coordinates of point 1. . . .	X_1, Y_1
Measured coordinates of point 2	X_2, Y_2
Error in a measurement.	e
Subscripts identify the error. . .	e_ℓ, e_{x1}, etc.
Bias Component of error e	b
Subscripts identify the bias . . .	b_ℓ, b_{x1}, etc.
Random component of error e	ϵ
Subscripts identify the random component	$\epsilon_\ell, \epsilon_{x1}$, etc.
Expected value of the random error. . .	σ
Subscripts identify the expected value.	σ_ℓ, σ_{x1}, etc.
Variance.	$\sigma_{\ell\ell} \equiv \sigma_\ell^2$ $\sigma_{x1\,x1} \equiv \sigma_{x1}^2$
Covariance.	$\sigma_{x1\,x2}, \sigma_{x1\,y1}$, etc.
Angle between two lines	θ
Angle of a line with the x-axis	$\theta_\ell, \theta_{1,2}, \theta_{1,3}$, etc.
Partial derivatives of a function . . .	f
$\frac{\partial f}{\partial x}$	f_1
$\partial f / \partial y$	f_2

APPENDIX A
DERIVATION OF ERRORS IN COMPUTED LENGTH

LET $\hat{\ell}$ - HAT, $\hat{\ell}$, BE THE COMPUTED LENGTH OF THE LINE, ℓ, AS DETERMINED FROM COORDINATE MEASUREMENTS OF POINT 1 AND POINT 2, THE END POINTS OF THE LINE.

THEN $$\hat{\ell} = \left[(X2 - X1)^2 + (Y2 - Y1)^2\right]^{\frac{1}{2}}$$

AND $$\ell = \left[(x2 - x1)^2 + (y2 - y1)^2\right]^{\frac{1}{2}}$$

BUT $$X1 = x1 + e_{x1}, \quad X2 = x2 + e_{x2}$$

$$Y1 = y1 + e_{y1}, \quad Y2 = y2 + e_{y2}$$

SUBSTITUTING

$$\hat{\ell} = \left[(x2 - x1 + e_{x2} - e_{x1})^2 + (y2 - y1 + e_{y2} - e_{y1})^2\right]^{\frac{1}{2}}$$

THE TERMS OF A TAYLOR SERIES EXPANSION ARE

$$f_0 = \left[(x_2 - x_1)^2 + (y_2 - y_1)^2 \right]^{\frac{1}{2}}$$

$$f_1 = \frac{\partial f}{\partial x} (e_{x_2} - e_{x_1}) = \frac{(x_2 - x_1)(e_{x_2} - e_{x_1})}{\left[(x_2 - x_1)^2 + (y_2 - y_1)^2 \right]^{\frac{1}{2}}}$$

$$f_2 = \frac{\partial f}{\partial y} (e_{y_2} - e_{y_1}) = \frac{(y_2 - y_1)(e_{y_2} - e_{y_1})}{\left[(x_2 - x_1)^2 + (y_2 - y_1)^2 \right]^{\frac{1}{2}}}$$

$$f_{11} = \frac{\partial^2 f}{\partial x^2} \frac{(e_{x_1} - e_{x_2})^2}{2!} = \frac{(e_{x_1} - e_{x_2})^2}{2!} \cdot$$

$$\frac{\left[(x_2 - x_1)^2 + (y_2 - y_1)^2 \right]^{\frac{1}{2}} - (x_2 - x_1)^2 \left[(x_2 - x_1)^2 + (y_2 - y_1)^2 \right]^{-\frac{1}{2}}}{(x_2 - x_1)^2 + (y_2 - y_1)^2}$$

LET θ_l BE THE ANGLE OF THE LINE WITH THE X-AXIS.

THEN

$$f_0 = \ell$$

$$f_1 = (\cos\theta_\ell)(e_{x2} - e_{x1})$$

$$f_2 = (\sin\theta_\ell)(e_{y2} - e_{y1})$$

$$f_{11} = \frac{1}{2}(\cos^2\theta_\ell)\frac{(e_{x1} - e_{x2})^2}{\ell}$$

IF THE ERROR IS SMALL COMPARED TO THE MEASURED LENGTH, THEN THE ERROR SQUARED IS VERY SMALL AND CAN BE NEGLECTED.

THUS $\hat{\ell} \doteq f + f_1 + f_2$

$$\hat{\ell} \doteq \ell + (\cos\theta_\ell)(e_{x2} - e_{x1}) + (\sin\theta_\ell)(e_{y2} - e_{y1})$$

THE ERRORS, e, ARE COMPOSED OF BOTH BIAS, b, AND RANDOM, ϵ, ERRORS.

THUS $\epsilon_\ell = b_\ell + \epsilon_\ell$

AND $\hat{\ell} = \ell + b_\ell + \epsilon_\ell$

THE EXPECTED VALUE, $E\hat{\ell}$, OF A LARGE NUMBER OF MEASUREMENTS, THE MEAN, $\mu_{\hat{\ell}}$, WILL BE THE TRUE VALUE PLUS THE BIAS. THUS

$$E\hat{\ell} = \ell + (\cos\theta_\ell)(b_{x2} - b_{x1}) + (\sin\theta_\ell)(b_{y2} - b_{y1})$$

THE BIAS ERROR IS

$$b'_\ell = (\cos\theta_\ell)(b_{x2} - b_{x1}) + (\sin\theta_\ell)(b_{y2} - b_{y1})$$

THE RANDOM COMPONENT IS THE MEASUREMENT MINUS THE MEAN.

$$\hat{\ell} - E\hat{\ell} = (\cos\theta_\ell)(\epsilon_{x2} - \epsilon_{x1}) + (\sin\theta_\ell)(\epsilon_{y2} - \epsilon_{y1})$$

THE VARIANCE, $\sigma^2_{\hat{\ell}}$, IS THE

EXPECTED VALUE OF THE SQUARE OF THE RANDOM COMPONENT.

$$\sigma_{\vec{P}}^2 = E\left(\vec{P} - M_{\vec{P}}\right)^2 \equiv \sigma_{\vec{P}\vec{P}}$$

$$\sigma_{\vec{P}\vec{P}} = \left(\cos^2\theta_{\vec{P}}\right)\left(\sigma_{x_2x_2} + \sigma_{x_1x_1} - 2\sigma_{x_1x_2}\right)$$
$$+ \left(\sin^2\theta_{\vec{P}}\right)\left(\sigma_{y_2y_2} + \sigma_{y_1y_1} - 2\sigma_{y_1y_2}\right)$$
$$+ 2\left(\sin\theta_{\vec{P}}\right)\left(\cos\theta_{\vec{P}}\right)\left(\sigma_{x_2y_2} + \sigma_{x_1y_1} - \sigma_{x_2y_1} - \sigma_{x_1y_2}\right)$$

ASSUME:

(a) VARIANCES ARE APPROXIMATELY EQUAL, σ_c^2, AND THERE IS NO CORRELATION. THEN

$$\sigma_{\vec{P}} = \sqrt{2}\,\sigma_c$$

(b) VARIANCES AND COVARIANCES ARE EQUAL, σ_c^2, AND THERE IS STRONG POSITIVE CORRELATION.

THEN $\sigma_A = 0$

(c) VARIANCES AND COVARIANCES ARE EQUAL, σ_c, AND THERE IS STRONG NEGATIVE CORRELATION THEN

$$\sigma_A = 2\sigma_c$$

APPENDIX B

DERIVATION OF ERRORS IN COMPUTED ANGLE AND AREA

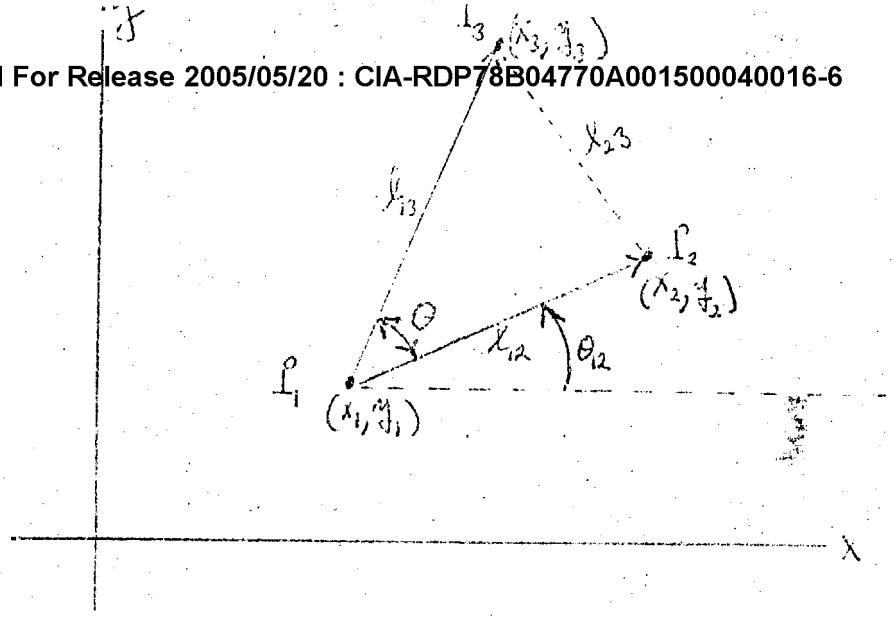

If $(x_1, y_1), (x_2, y_2), (x_3, y_3)$ are the cartesian coordinates of three points, then the angle θ (measured in radians) indicated in the above figure is

$$(1.1) \qquad \theta = \operatorname{Arc\,Cos}\left\{ \frac{(x_3 - x_1)(x_2 - x_1) + (y_3 - y_1)(y_2 - y_1)}{\left[(x_3 - x_1)^2 + (y_3 - y_1)^2\right]^{1/2} \left[(x_2 - x_1)^2 + (y_2 - y_1)^2\right]^{1/2}} \right\}.$$

(By convention $0 \le \theta \le \pi$, i.e. the angle θ is between 0° and 180°.)

Consider the directed line segments (vectors) $\overrightarrow{P_1P_2}$ and $\overrightarrow{P_1P_3}$, and let

$$(1.2) \qquad \overrightarrow{P_1P_2} = (\ell_{12}\cos\theta_{12},\ \ell_{12}\sin\theta_{12}),$$
$$\overrightarrow{P_1P_3} = (\ell_{13}\cos\theta_{13},\ \ell_{13}\sin\theta_{13}).$$

Thus, for example ℓ_{12} is the length of the line segment $\overrightarrow{P_1P_2}$ and θ_{12} is the angle that the line segment $\overrightarrow{P_1P_2}$ makes with the X axis. (The angles θ_{12} and θ_{13} may range between 0 and 2π.)

Let $(e_{x_1}, e_{y_1}, e_{x_2}, e_{y_2}, e_{x_3}, e_{y_3})$ denote the errors in "measuring" $(x_1, y_1, x_2, y_2, x_3, y_3)$.

Set

$$(1.3) \qquad E(e_{x_1}, e_{y_1}, e_{x_2}, e_{y_2}, e_{x_3}, e_{y_3}) \equiv (\beta_{x_1}, \beta_{y_1}, \beta_{x_2}, \beta_{y_2}, \beta_{x_3}, \beta_{y_3}).$$

The β's expressed above are the biases in the coordinate measurements.

Let

$$(1.4)\quad (\epsilon_{x_1}, \epsilon_{y_1}, \epsilon_{x_2}, \epsilon_{y_2}, \epsilon_{x_3}, \epsilon_{y_3}) \equiv (e_{x_1}-\beta_{x_1}, e_{y_1}-\beta_{y_1}, \cdots, e_{x_3}-\beta_{x_3}, e_{y_3}-\beta_{y_3})$$

The ϵ's appearing above are the <u>random errors</u> in the coordinate measurements

Let the <u>covariance matrix</u> of the random errors be

$$(1.5)\quad \sum_{\epsilon} \equiv E \begin{bmatrix} \epsilon_{x_1} \\ \epsilon_{y_1} \\ \epsilon_{x_2} \\ \epsilon_{y_2} \\ \epsilon_{x_3} \\ \epsilon_{y_3} \end{bmatrix} \begin{bmatrix} \epsilon_{x_1}, \epsilon_{y_1}, \cdots, \epsilon_{x_3}, \epsilon_{y_3} \end{bmatrix} \equiv \begin{bmatrix} \sigma_{x_1x_1} & \sigma_{x_1y_1} & \cdots & \sigma_{x_1x_3} & \sigma_{x_1y_3} \\ \sigma_{y_1x_1} & \sigma_{y_1y_1} & & & \vdots \\ \vdots & & & & \\ & & (\text{etc.}) & & \\ \sigma_{x_3x_1} & & & \sigma_{x_3x_3} & \sigma_{x_3y_3} \\ \sigma_{y_3x_1} & \cdots & \cdots & \cdots & \sigma_{y_3y_3} \end{bmatrix}$$

Let $\hat{\theta}$ denote a "determination" of the angle θ calculated using Eq (1.1) <u>with</u> the errors $e_{x_1}, e_{y_1}, e_{x_2}, e_{y_2}, e_{x_3}, e_{y_3}$ in the coordinates. To first order (in a Taylor series expansion) the resulting error in $\hat{\theta}$ is then given by

$$(1.6)\quad e_\theta = \left(\frac{\sin\theta_{12}}{\ell_{12}}\right)(e_{x_2}-e_{x_1}) - \left(\frac{\cos\theta_{12}}{\ell_{12}}\right)(e_{y_2}-e_{y_1}) - \left(\frac{\sin\theta_{13}}{\ell_{13}}\right)(e_{x_3}-e_{x_1}) + \left(\frac{\cos\theta_{13}}{\ell_{13}}\right)(e_{y_3}-e$$

The <u>bias error</u> is therefore

$$(1.7)\quad \beta_\theta = \left(\frac{\sin\theta_{12}}{\ell_{12}}\right)(\beta_{x_2}-\beta_{x_1}) - \left(\frac{\cos\theta_{12}}{\ell_{12}}\right)(\beta_{y_2}-\beta_{y_1}) - \left(\frac{\sin\theta_{13}}{\ell_{13}}\right)(\beta_{x_3}-\beta_{x_1}) + \left(\frac{\cos\theta_{13}}{\ell_{13}}\right)(\beta_{y_3}-\beta_{y_1})$$

The <u>random error</u> is

$$(1.8)\quad \epsilon_\theta = \left(\frac{\sin\theta_{12}}{\ell_{12}}\right)(\epsilon_{x_2}-\epsilon_{x_1}) - \left(\frac{\cos\theta_{12}}{\ell_{12}}\right)(\epsilon_{y_2}-\epsilon_{y_1}) - \left(\frac{\sin\theta_{13}}{\ell_{13}}\right)(\epsilon_{x_3}-\epsilon_{x_1}) + \left(\frac{\cos\theta_{13}}{\ell_{13}}\right)(\epsilon_{y_3}-\epsilon_{y_1})$$

The variance σ_θ^2 of the random error ϵ_θ is

$$(1.9) \qquad \sigma_\theta^2 \equiv E\,\epsilon_\theta^2 .$$

Upon using Eqs. (1.8) and (1.5) one obtains the following general expression for the variance σ_θ^2:

$$(1.10) \qquad \sigma_\theta^{-2} = \begin{bmatrix} \left(\frac{\sin\theta_{12}}{\ell_{12}} + \frac{\sin\theta_{13}}{\ell_{13}}\right) \\ \left(\frac{\cos\theta_{12}}{\ell_{12}} - \frac{\cos\theta_{13}}{\ell_{13}}\right) \\ \frac{\sin\theta_{12}}{\ell_{12}} \\ -\frac{\cos\theta_{12}}{\ell_{12}} \\ -\frac{\sin\theta_{13}}{\ell_{13}} \\ \frac{\cos\theta_{13}}{\ell_{13}} \end{bmatrix}' \begin{bmatrix} \sigma_{x_1x_1} & \sigma_{x_1y_1} & \cdots & \sigma_{x_1y_3} \\ \vdots & & & \vdots \\ & \text{etc.} & & \\ \sigma_{x_3x_3} & \sigma_{x_3y_3} & & \\ \sigma_{y_3x_1} & \cdots & \sigma_{y_3x_3} & \sigma_{y_3y_3} \end{bmatrix} \begin{bmatrix} \left(\frac{-\sin\theta_{12}}{\ell_{12}} + \frac{\sin\theta_{13}}{\ell_{13}}\right) \\ \left(\frac{\cos\theta_{12}}{\ell_{12}} - \frac{\cos\theta_{13}}{\ell_{13}}\right) \\ \frac{\sin\theta_{12}}{\ell_{12}} \\ -\frac{\cos\theta_{12}}{\ell_{12}} \\ -\frac{\sin\theta_{13}}{\ell_{13}} \\ \frac{\cos\theta_{13}}{\ell_{13}} \end{bmatrix}$$

Example: If in (1.10) all the covariances are zero (i.e. the random errors are all uncorrelated) and $\sigma_{x_1x_1} = \sigma_{y_1y_1} = \sigma_{x_2x_2} = \sigma_{y_2y_2} = \sigma_{x_3x_3} = \sigma_{y_3y_3} \equiv \sigma_c^2$ (i.e. all the random coordinate errors have a common variance σ_c^2) then

$$(1.11) \qquad \sigma_\theta^2 = \left[\left(\frac{-\sin\theta_{12}}{\ell_{12}} + \frac{\sin\theta_{13}}{\ell_{13}}\right)^2 + \left(\frac{\cos\theta_{12}}{\ell_{12}} - \frac{\cos\theta_{13}}{\ell_{13}}\right)^2 + \frac{\sin^2\theta_{12}}{\ell_{12}^2} + \frac{\cos^2\theta_{12}}{\ell_{12}^2} + \frac{\sin^2\theta_{13}}{\ell_{13}^2} + \frac{\cos^2\theta_{13}}{\ell_{13}^2}\right]\sigma_c^2$$

$$= \left[\frac{2}{\ell_{12}^2} + \frac{2}{\ell_{13}^2} - \frac{2}{\ell_{12}\ell_{13}}\left(\sin\theta_{12}\sin\theta_{13} + \cos\theta_{12}\cos\theta_{13}\right)\right]\sigma_c^2$$

$$= 2\left[\frac{1}{\ell_{12}^2} + \frac{1}{\ell_{13}^2} - \frac{1}{\ell_{12}\ell_{13}}\cos(\theta_{13} - \theta_{12})\right]\sigma_c^2$$

$$= 2\left[\frac{1}{\ell_{12}^2} + \frac{1}{\ell_{13}^2} - \frac{\cos\theta}{\ell_{12}\ell_{13}}\right]\sigma_c^2 .$$

STAT

9/30/67

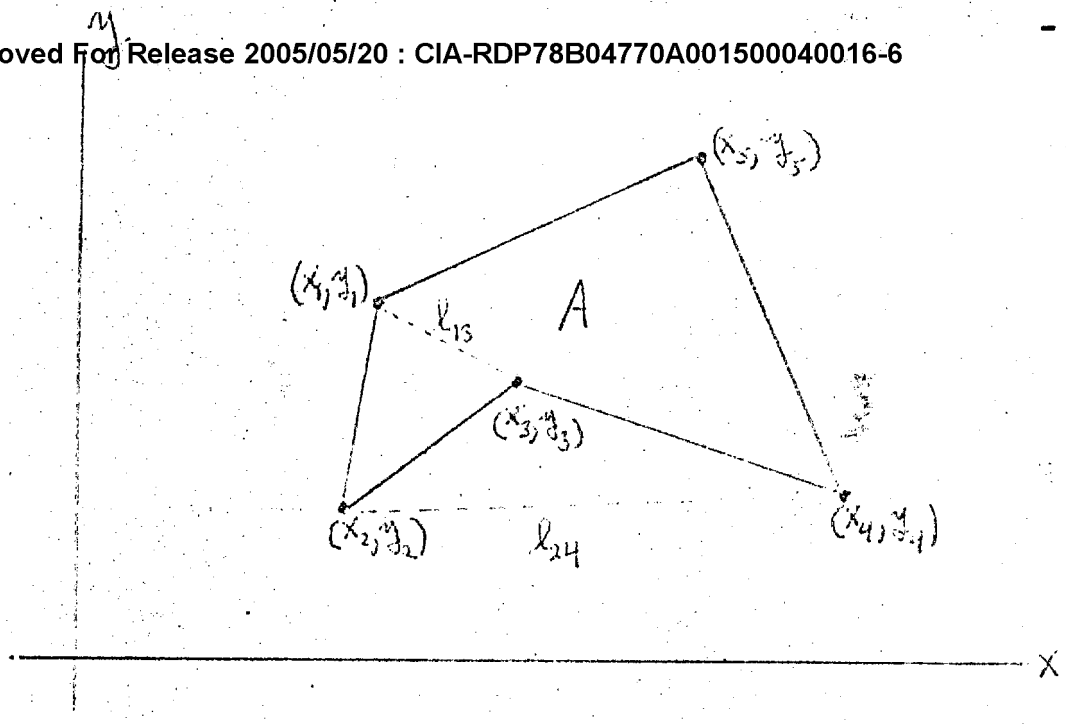

Consider a simple closed polygon. Traversing the boundary counter-clockwise, let the vertices of the polygon be numbered consecutively $1, 2, \cdots, j, \cdots, n$. Let the cartesian coordinates of the j-th vertex be (x_j, y_j). In the above figure and the formulae given below corresponding to it $n = 5$. It will be clear how the results for $n = 5$ extend to a general value of n. Let A denote the area of the polygon.

For $n = 5$,

$$(2.1)\quad A = \frac{1}{2}\left[(x_1 - x_2)(y_1 + y_2) + (x_2 - x_3)(y_2 + y_3) + (x_3 - x_4)(y_3 + y_4) + (x_4 - x_5)(y_4 + y_5) - (x_5 - x_1)(y_5 + y_1)\right].$$

In general

$$(2.2)\quad A = \frac{1}{2}\sum_{j=1}^{n}(x_j - x_{j+1})(y_j + y_{j+1})$$

where subscript values are understood to be taken modulo n. [For example, (x_{n+1}, y_{n+1}) is (x_1, y_1).]

Let (e_{x_j}, e_{y_j}) $j = 1, 2, \cdots, n$ denote as before errors in measuring the respective coordinates (x_j, y_j).

Let

$$(2.3) \qquad E\,(e_{x_j}, e_{y_j}) \equiv (\beta_{x_j}, \beta_{y_j}), \quad j = 1, 2, \cdots, n .$$

The β's in Eq. (2.3) denote the biases in the coordinate measurements.

Let

$$(2.4) \qquad (e_{x_j}, e_{y_j}) \equiv (e_{x_j} - \beta_{x_j}, e_{y_j} - \beta_{y_j}), \quad j = 1, 2, \cdots, n .$$

The e's in Eq. (2.4) are the random errors in the coordinate measurement. If the covariance matrix of these random errors be denoted by Σ_ϵ,

$$(2.5) \qquad \Sigma_\epsilon = \begin{bmatrix} e_{x_1} \\ e_{y_1} \\ \vdots \\ e_{x_n} \\ e_{y_n} \end{bmatrix} \begin{bmatrix} e_{x_1}, e_{y_1}, \cdots, e_{x_n}, e_{y_n} \end{bmatrix} = \begin{bmatrix} \sigma_{x_1 x_1} & \sigma_{x_1 y_1} & & \text{etc.} \\ \sigma_{y_1 x_1} & \sigma_{y_1 y_1} & & \\ & & & \\ \text{etc.} & & & \end{bmatrix}$$

$$\begin{bmatrix} \sigma_{x_j x_k} & \sigma_{x_j y_k} \\ \sigma_{y_j x_k} & \sigma_{y_j y_k} \end{bmatrix}$$

Let $\hat{A}$ denote a "determination" of the area A calculated using Eq. (2.2) with the errors (e_{x_j}, e_{y_j}), $j = 1, 2, \cdots, n$ in the respective coordinates. For $n = 5$, the resulting error $e_A \equiv \hat{A} - A$ is then given by

$$(2.6) \qquad e_A = \frac{1}{2}\Big[(y_2 - y_5)e_{x_1} - (x_2 - x_5)e_{y_1} + (y_3 - y_1)e_{x_2} - (x_3 - x_1)e_{y_2} + (y_4 - y_2)e_{x_3} - (x_4 - x_2)e_{y_3} + (y_5 - y_3)e_{x_4} - (x_5 - x_3)e_{y_4} + (y_1 - y_4)e_{x_5} - (x_1 - x_4)e_{y_5}\Big] .$$

In general

$$(2.7) \qquad e_A = \frac{1}{2}\sum_{j=1}^{n}\Big[(y_{j+1} - y_{j-1})e_{x_j} - (x_{j+1} - x_{j-1})e_{y_j}\Big],$$

where subscripts with j appearing are taken modulo n. [For example, (x_0, y_0) is $(x_n$ and (e_{x_0}, e_{y_0}) is (e_{x_n}, e_{y_n}).]

The *bias error* is in general therefore

$$(2.8) \qquad \beta_A = \frac{1}{2}\sum_{j=1}^{n}\left[(y_{j+1}-y_{j-1})\beta_{x_j} - (x_{j+1}-x_{j-1})\beta_{y_j}\right].$$

The *random error* is in general

$$(2.9) \qquad \epsilon_A = \frac{1}{2}\sum_{j=1}^{n}\left[(y_{j+1}-y_{j-1})\epsilon_{x_j} - (x_{j+1}-x_{j-1})\epsilon_{y_j}\right],$$

The *variance* σ_A^2 of the random error ϵ_A is

$$(2.10) \qquad \sigma_A^2 \equiv E\,\epsilon_A^2 .$$

Upon using Eqs. (2.9) and (2.5) one obtains the following general expression for the variance σ_A^2:

$$(2.11) \qquad \sigma_A^2 = \frac{1}{4}\begin{bmatrix}(y_2-y_n)\\ -(x_2-x_n)\\ (y_3-y_1)\\ -(x_3-x_1)\\ \vdots\\ (y_1-y_{n-1})\\ -(x_1-x_{n-1})\end{bmatrix}^{\prime}\begin{bmatrix}\begin{matrix}\sigma_{x_1x_1} & \sigma_{x_1y_1}\\ \sigma_{y_1x_1} & \sigma_{y_1y_1}\end{matrix} & & \text{etc.}\\ & \ddots & \\ \text{etc.} & & \begin{matrix}\sigma_{x_jx_k} & \sigma_{x_jy_k}\\ \sigma_{y_jx_k} & \sigma_{y_jy_k}\end{matrix}\end{bmatrix}\begin{bmatrix}(y_2-y_n)\\ -(x_2-x_n)\\ (y_3-y_1)\\ -(x_3-x_1)\\ \vdots\\ (y_1-y_{n-1})\\ -(x_1-x_{n-1})\end{bmatrix}$$

Example: If in (2.11) all the covariances are zero (i.e. the random errors [illegible]) and $\sigma_{x_1x_1} = \sigma_{y_1y_1} = \sigma_{x_2x_2} = \sigma_{y_2y_2} = \ldots = \sigma_{x_nx_n} = \sigma_{y_ny_n} = \sigma_c^2$

(i.e. all the random variables have a common variance σ_c^2)

then

$$(2.12)\quad \sigma_A^2 = \frac{1}{4}\left[(y_2-y_m)^2+(x_2-x_n)^2+(y_3-y_1)^2+(x_3-x_1)^2+\cdots+(y_1-y_{n-1})^2+(x_1-x_{n-1})^2\right]\sigma_c^2$$

$$= \frac{1}{4}\left[\ell_{m2}^2+\ell_{13}^2+\cdots+\ell_{n-1,1}^2\right]\sigma_c^2$$

where ℓ_{jk} denotes the length of the line segment connecting vertex j with vertex k.

[redacted] STAT

9/30/67

APPENDIX C

DERIVATION OF GENERAL FORMULA OF ERRORS IN APPLYING CORRECTION FACTORS

Let X and Y be corrected coordinates after some corrections such as optical distortion have been applied to coordinate measurements. Then

$$X = f(x + e_x, y + e_y)$$

$$Y = g(x + e_x, y + e_y)$$

To a first order accuracy in a Taylor Series expansion:

$$\begin{vmatrix} X \\ Y \end{vmatrix} = \begin{vmatrix} f(x,y) \\ g(x,y) \end{vmatrix} + \begin{vmatrix} f_1 & f_2 \\ g_1 & g_2 \end{vmatrix}_{x,y} \begin{vmatrix} e_x \\ e_y \end{vmatrix}$$

Since the total error, e, in a coordinate measurement is composed of bias error b, and random error, ϵ, the bias error B_X, B_Y of the corrected coordinates will be

$$\begin{vmatrix} B_X \\ B_Y \end{vmatrix} = \begin{vmatrix} f_1 & f_2 \\ g_1 & g_2 \end{vmatrix}_{x,y} \begin{vmatrix} b_x \\ b_y \end{vmatrix}$$

and the random error ϵ_X, ϵ_Y, of the corrected coordinates will be

$$\begin{vmatrix} \epsilon_X \\ \epsilon_Y \end{vmatrix} = \begin{vmatrix} f_1 & f_2 \\ g_1 & g_2 \end{vmatrix}_{x,y} \begin{vmatrix} \epsilon_x \\ \epsilon_y \end{vmatrix}$$

The expected value E of the transformed random errors ϵ_x, ϵ_y, is the covariance matrix. Thus

$$E \begin{vmatrix} \epsilon_x \\ \epsilon_y \end{vmatrix} \begin{vmatrix} \epsilon_x & \epsilon_y \end{vmatrix} = \begin{vmatrix} \sigma_{xx} & \sigma_{xy} \\ \sigma_{yx} & \sigma_{yy} \end{vmatrix}$$

$$\begin{vmatrix} \sigma_{XX} & \sigma_{XY} \\ \sigma_{YX} & \sigma_{YY} \end{vmatrix} = \begin{vmatrix} f_1 & f_2 \\ g_1 & g_2 \end{vmatrix} \begin{vmatrix} f_1 & g_1 \\ f_2 & g_2 \end{vmatrix} E \begin{vmatrix} \epsilon_x \\ \epsilon_y \end{vmatrix} \begin{vmatrix} \epsilon_x & \epsilon_y \end{vmatrix}$$

But $E(\epsilon_x^2) = \sigma_{xx}$, $E(\epsilon_y^2) = \sigma_{yy}$ etc.

$$\begin{vmatrix} \sigma_{XX} & \sigma_{XY} \\ \sigma_{YX} & \sigma_{YY} \end{vmatrix} = \begin{vmatrix} f_1 & f_2 \\ g_1 & g_2 \end{vmatrix} \cdot \begin{vmatrix} \sigma_{xx} f_1 + \sigma_{xy} f_2 & \sigma_{xx} g_1 + \sigma_{xy} g_2 \\ \sigma_{yx} f_1 + \sigma_{yy} f_2 & \sigma_{yx} g_1 + \sigma_{yy} g_2 \end{vmatrix}$$

Thus the transformed variances σ_{XX} and σ_{YY} are

$$\sigma_{XX} = f_1^2 \sigma_{xx} + 2 \sigma_{xy} f_1 f_2 + f_2^2 \sigma_{yy}$$

$$\sigma_{YY} = g_1^2 \sigma_{xx} + 2 \sigma_{xy} g_1 g_2 + g_2^2 \sigma_{yy}$$

etc. for the other terms of the covariance matrix.

Thus we see that in the transformation from coordinates x,y, to new corrected coordinates X,Y,

the transformed errors are functions of the partial derivatives of the original functions. Unless the error transformation is carefully considered, it is possible to make a correction which increases rather than decreases errors.

APPENDIX D

DEFINITION OF BIAS ERROR AND RANDOM ERROR

A measurement, $\hat{l}$, of a linear dimension can be considered to be composed of the true length, l, the bias error, b, and the random error, ϵ, as shown in Fig. 10.

Precision refers to how closely grouped a number of measurements are about the mean value of the measurements. Precision can be characterized by the rms deviation of the measurements about the mean. If the measurements are normally distributed about a mean, then the rms value will be one standard deviation.

Accuracy refers to how close a measurement is to the true value and includes bias error as well as random error. Accuracy can only be determined if either true length or bias error are known. In establishing procedures to measure the distance between two points, it is advantageous if the bias errors can be made to cancel.

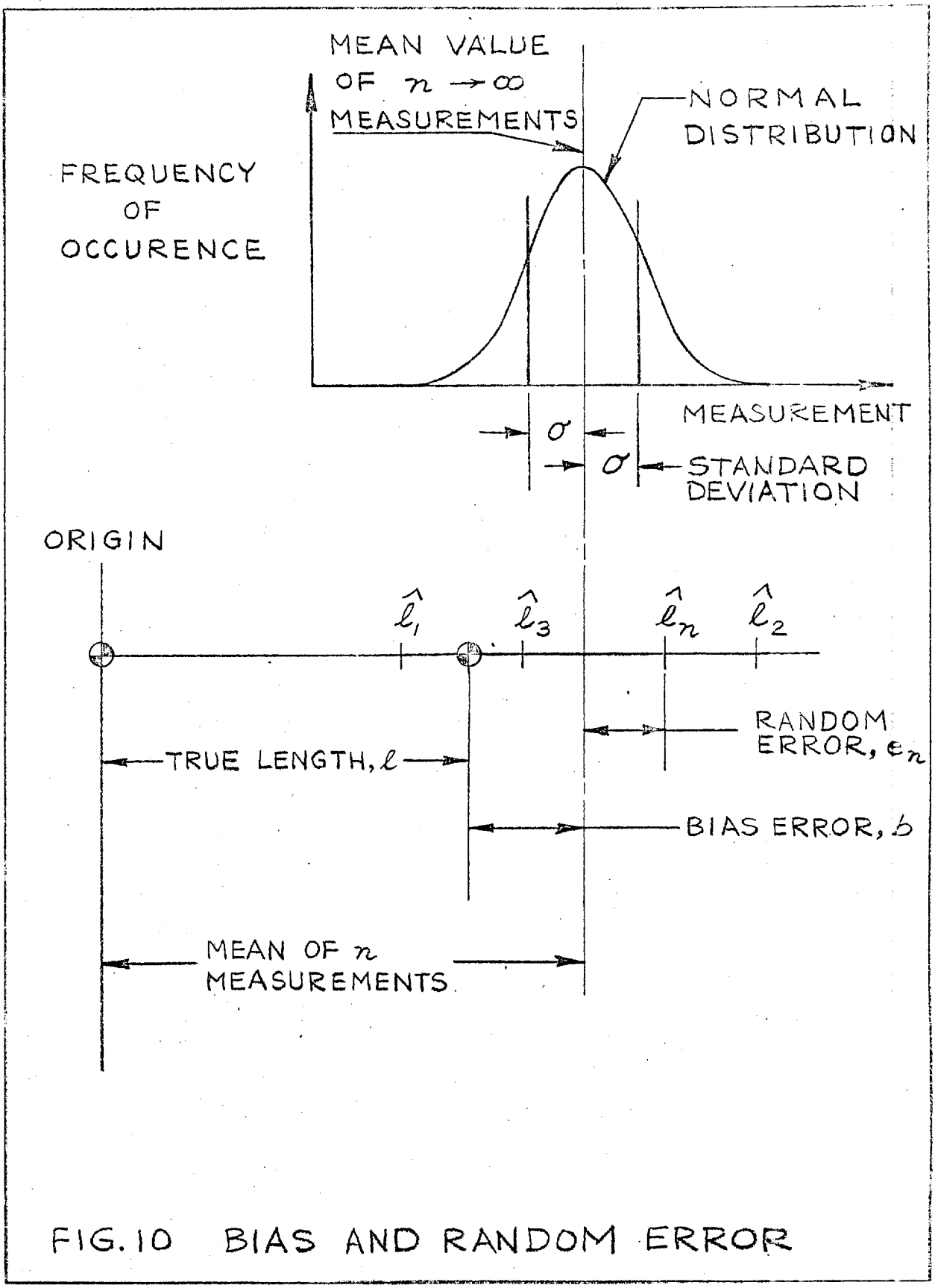

FIG. 10 BIAS AND RANDOM ERROR